Supporting Information

Dynamic Chirality in the Mechanism of Action of Allosteric CD36 Modulators of Macrophage-Driven Inflammation

Emma Danelius,[‖,†] Ragnhild G. Ohm,[‡] Ahsanullah,[‡] Mukandila Mulumba,[§] Huy Ong,[§] Sylvain Chemtob,[‖] Mate Erdelyi[⊥,°] and William D. Lubell[‡,*]

[‡]Département de Chimie, ◊Département de Pédiatrie, et §Faculté de Pharmacie, Universite de Montreal, CP 6128, Station Centre-ville, Montreal, Quebec H3C3J7, Canada

[§]Faculty of Pharmacy, University of Montreal, Montréal, Québec H3T1J4, Canada

[‖]Department of Pediatrics, Centre Hospitalier Universitaire (CHU) Sainte - Justine Research Center, Montréal, Québec H3T1C5, Canada

[⊥]Department of Chemistry – BMC, Uppsala University, Husargatan 3, SE-752 37 Uppsala, Sweden

[°]The Swedish NMR Centre, Medicinaregatan 5, SE-413 90 Gothenburg, Sweden.

[£]Current address: Department of Chemistry, Quaid-i-Azam University, Islamabad 45320, Pakistan

Contents

Synthetic Procedures

For synthetic procedure of aza-peptide **1**, **10** and **11**, see[1].

Solid Phase Chemistry

Fmoc-based peptide synthesis was performed on an automated shaker using polystyrene Rink amide resin. Couplings of amino acids (3 equiv.) were performed in DMF using DIC (3 equiv.) and HOBt (3 equiv.) for 3–6 hours. Fmoc-deprotections were performed by treating the resin with 20% piperidine in DMF for 30 min. The resin was washed after each coupling and deprotection step sequentially with DMF (×3), MeOH (×3) THF (×3) and CH_2Cl_2 (×3).

Fmoc-Lys(allyl, *o*-NBS)-resin, 3

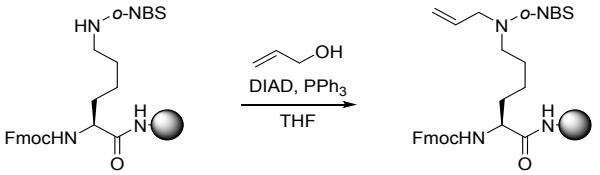

3: Vacuum dried Fmoc-Lys(*o*-NBS)-resin **4** (0.441 mmol) was placed in a syringe fitted with a Teflon™ filter, suspended in THF (dry, 5 mL) and treated sequentially with solutions of allyl alcohol (206 µL, 3.03 mmol) in THF (dry, 1 mL), PPh_3 (397 mg, 1.51 mmol) in THF (dry, 1 mL), and DIAD (298 µL, 1.51 mmol) in THF (dry, 1 mL). The mixture in the syringe was shaken for 90 min. The resin was filtered and sequentially washed with DMF (×3), MeOH (×3), THF (×3) and CH_2Cl_2 (×3). Examination by LCMS of a cleaved resin sample (5 mg) showed complete allylation: LCMS (30–95% MeOH containing 0.1% formic acid in water containing 0.1% formic acid over 10 min) R_t = 8.65 min. ESI-MS *m/z*: calcd for $C_{30}H_{33}N_4O_7S^+$ $[M+H]^+$ 593.2, found 593.2.

Fmoc-Lys(*o*-NBS)-resin, 4

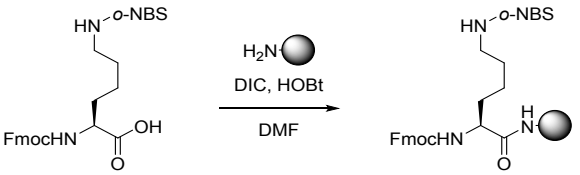

4: On Rink amide resin (3.00 g) in a syringe fitted with a Teflon™ filter, Fmoc removal was performed by treating the resin with a solution of 20% piperidine in DMF over 30 min. The resin was filtered and washed sequentially with DMF (×3), MeOH (×3) and CH_2Cl_2 (×3). Fmoc-Lys(*o*-NBS)-OH (1.62 g, 2.93 mmol) was dissolved in DMF (20 mL) and treated with DIC (0.7 mL, 4.52 mmol) and HOBt (611 mg, 4.52 mmol), stirred for 3 min. and added to the syringe containing the resin. The mixture was shaken for 14 hours. The resin was then filtered and sequentially washed with DMF (×3), MeOH (×3) and CH_2Cl_2 (×3).

Boc-Ala-D-Pra-D-Trp(Boc)-Ala-Trp(Boc)-D-Phe-Lys(allyl, *o*-NBS)-resin, 5a

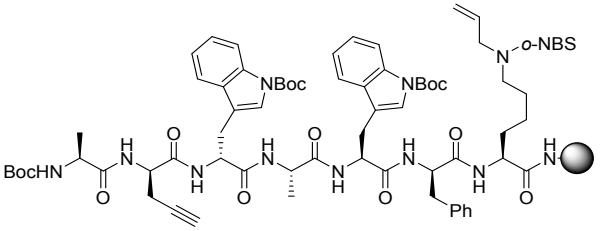

5a: LCMS (30–95% MeOH containing 0.1% formic acid in water containing 0.1% formic acid over 10 min) R_t = 6.48 min. ESI-MS *m/z*: calcd for $C_{57}H_{67}N_{12}O_{11}S^+$ $[M+H]^+$ 1127.5, found 1127.5.

Boc-Ala-Pra-D-Trp(Boc)-Ala-Trp(Boc)-D-Phe-Lys(allyl, *o*-NBS)-resin, 5b

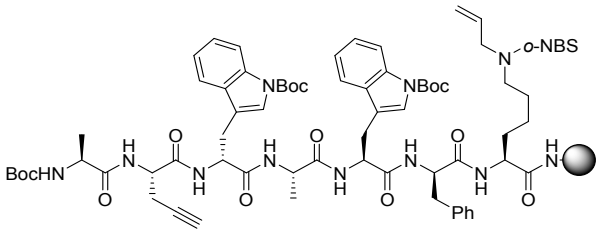

5b: LCMS (30–95% MeOH containing 0.1% formic acid in water containing 0.1% formic acid over 10 min) R_t = 6.66 min. ESI-MS *m/z*: calcd for $C_{57}H_{67}N_{12}O_{11}S^+$ $[M+H]^+$ 1127.5, found 1127.5.

Boc-Ala-D-Pra-Ala-Trp(Boc)-D-Phe-Lys(allyl, *o*-NBS)-resin, 5c

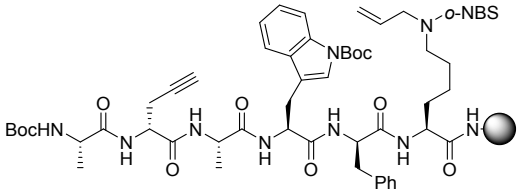

5c: LCMS (30–95% MeOH containing 0.1% formic acid in water containing 0.1% formic acid over 10 min) R_t = 5.73 min. ESI-MS *m/z*: calcd for $C_{46}H_{57}N_{10}O_{10}S^+$ $[M+H]^+$ 941.4, found 941.4.

Boc-Ala-Pra-Ala-Trp(Boc)-D-Phe-Lys(allyl, *o*-NBS)-resin, 5d

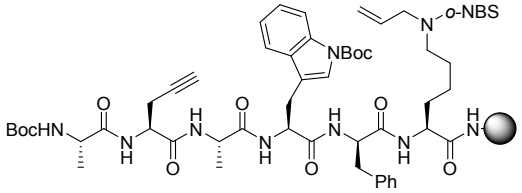

5d: LCMS (30–95% MeOH containing 0.1% formic acid in water containing 0.1% formic acid over 10 min) R_t = 5.77 min. ESI-MS *m/z*: calcd for $C_{46}H_{57}N_{10}O_{10}S^+$ $[M+H]^+$ 941.4, found 941.4.

Boc-Ala-D-Pra-D-Trp(Boc)-Ala-Trp(Boc)-D-Phe-Lys(allyl)-resin, 6a

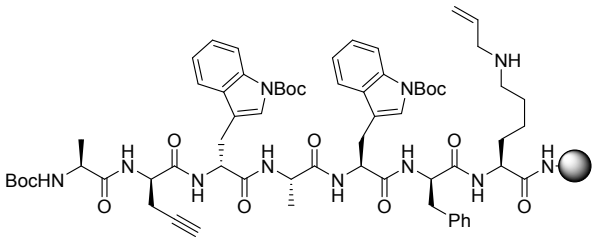

6a: *o*-NBS-protected heptapeptide **5a** (~300 mg, 0.10 mmol) in a syringe fitted with a Teflon™ filter was swollen in DMF (6 mL) and treated with DBU (150 µL, 1.00 mmol) and 2-mercaptoethanol (35 µL, 0.50 mmol). The mixture in the syringe was shaken for 1 h. The resin was filtered and sequentially washed with DMF (×3), MeOH (×3), THF (×3) and CH_2Cl_2 (×3). Examination by LCMS of a cleaved resin sample (5 mg) showed complete *o*-NBS-removal: LCMS (20–80% MeOH containing 0.1% formic acid in water containing 0.1% formic acid over 10 min) R_t = 4.79 min. ESI-MS *m/z*: calcd for $C_{51}H_{64}N_{11}O_7^+$ $[M+H]^+$ 942.5, found 942.5.

Boc-Ala-Pra-D-Trp(Boc)-Ala-Trp(Boc)-D-Phe-Lys(allyl)-resin, 6b

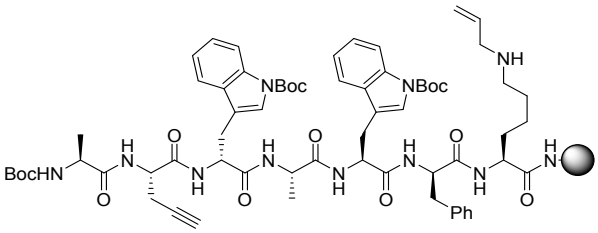

6b: *o*-NBS-protected heptapeptide **5b** (~300 mg, 0.09 mmol) in a syringe fitted with a Teflon™ filter was swollen in DMF (6 mL) and treated with DBU (130 µL, 0.87 mmol) and 2-mercaptoethanol (30 µL, 0.43 mmol). The mixture in the syringe was shaken for 1 h. The resin was filtered and sequentially washed with DMF (×3), MeOH (×3), THF (×3) and CH_2Cl_2 (×3). Examination by LCMS of a cleaved resin sample (5 mg) showed complete *o*-NBS-removal: LCMS (20–80% MeOH containing 0.1% formic acid in water containing 0.1% formic acid over 10 min) R_t = 5.05 min. ESI-MS *m/z*: calcd for $C_{51}H_{64}N_{11}O_7^+$ $[M+H]^+$ 942.5, found 942.5.

Boc-Ala-D-Pra-Ala-Trp(Boc)-D-Phe-Lys(allyl)-resin, 6c

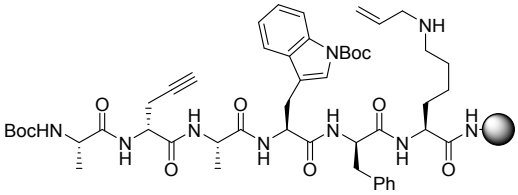

6c: *o*-NBS-protected hexapeptide **5c** (~600 mg, 0.156 mmol) in a syringe fitted with a Teflon™ filter was swollen in DMF (5 mL) and treated with DBU (210 µL, 1.40 mmol) and 2-mercaptoethanol (50 µL, 0.71 mmol). The mixture in the syringe was shaken for 1 h. The resin was filtered and sequentially washed with DMF (×3), MeOH (×3), THF (×3) and CH_2Cl_2 (×3). Examination by LCMS of a cleaved resin sample (5 mg) showed complete *o*-NBS-removal: LCMS (30–95% MeOH containing 0.1% formic acid in water containing 0.1% formic acid over 10 min) R_t = 1.50 min. ESI-MS *m/z*: calcd for $C_{40}H_{54}N_9O_6^+$ $[M+H]^+$ 756.4, found 756.4.

Boc-Ala-Pra-Ala-Trp(Boc)-D-Phe-Lys(allyl)-resin, 6d

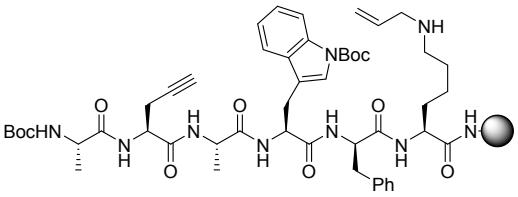

6d: *o*-NBS-protected hexapeptide **5d** (~600 mg, 0.14 mmol) in a syringe fitted with a Teflon™ filter was swollen in DMF (5 mL) and treated with DBU (210 µL, 1.40 mmol) and 2-mercaptoethanol (50 µL, 0.71 mmol). The mixture in the syringe was shaken for 1 h. The resin was filtered and sequentially washed with DMF (×3), MeOH (×3), THF (×3) and CH_2Cl_2 (×3). Examination by LCMS of a cleaved resin sample (5 mg) showed complete *o*-NBS-removal: LCMS (30–95% MeOH containing 0.1% formic acid in water containing 0.1% formic acid over 10 min) R_t = 1.51 min. ESI-MS *m/z*: calcd for $C_{40}H_{54}N_9O_6^+$ $[M+H]^+$ 756.4, found 756.4.

Ala-cyclo(D-Pra-D-Trp-Ala-Trp-D-Phe-Lys(allyl)), *R*-8

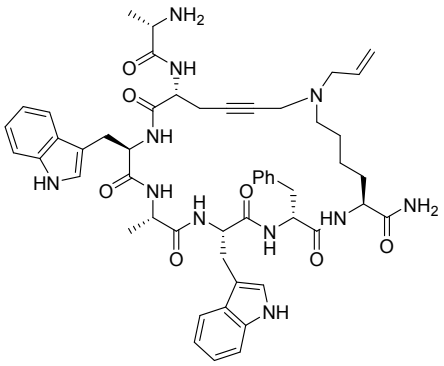

R-**8**: Heptapeptide resin **6a** (~300 mg, 0.10 mmol) was swollen in DMSO (5 mL) for 30 min in a syringe tube equipped with Teflon™ filter, and stopper, treated with CuI (4.0 mg, 0.02 mmol) and aqueous formaldehyde (50 µL, 0.69 mmol, 37% in H_2O), shaken on an automated shaker for 29 h, and filtered. After filtration, the resin was washed sequentially with AcOH/H_2O/DMF (5:15:80, v/v/v, ×3), DMF (×3), THF (×3), MeOH (×3), and DCM (×3). Examination by LCMS of a cleaved resin sample (5 mg) showed complete conversion, and a peak with molecular ion consistent with cyclic heptapeptide *R*-**8** was observed: MS *m/z*: calcd for $C_{52}H_{63}N_{11}NaO_7^+$ $[M+Na]^+$ 976.5, found 976.4.

Resin-bound cyclic peptide *R*-**8** was deprotected and cleaved from the support using a freshly made solution of TFA/H_2O/TES (95:2.5:2.5, v/v/v, 5 mL) at rt for 2 h. The resin was filtered and rinsed with TFA (5 mL). The filtrate and rinses were concentrated until a crude oil persisted, from which a precipitate was obtained by addition of cold ether (10 mL). After centrifugation (1200 rpm for 10 min), the supernatant was removed, and the crude peptide precipitate was taken up in aqueous MeOH (10% v/v) and freeze-dried prior to purification. The resulting light brown fluffy material was purified by preparative HPLC to give cyclic heptapeptide *R*-**8** (0.7 mg, 1%) as white fluffy material.

LCMS analysis of cyclic peptide *R*-**8** was performed using a linear gradient of a) 10–90% of MeOH containing 0.1% formic acid in H_2O (0.1% formic acid) over 10 min, then at 90% MeOH (0.1% formic acid) for 5 min, R_t = 5.80 min; b) 10–90% MeCN containing 0.1% formic acid in H_2O containing 0.1% formic acid over 10 min, then at 90% MeCN (0.1% formic acid) for 5 min, R_t = 4.24 min; HRMS *m/z*: calcd for $C_{52}H_{63}N_{11}NaO_7^+$ $[M+Na]^+$ 976.4804, found 976.4817.

HPLC chromatogram in solvent system a)

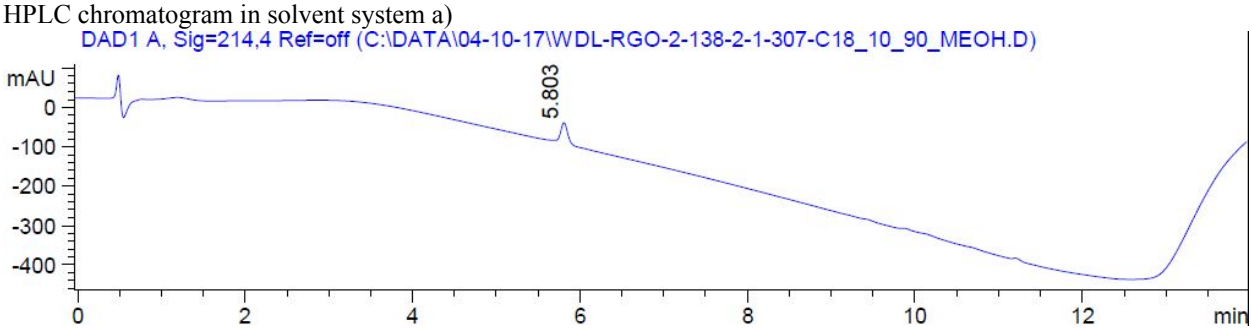

HPLC chromatogram in solvent system b)

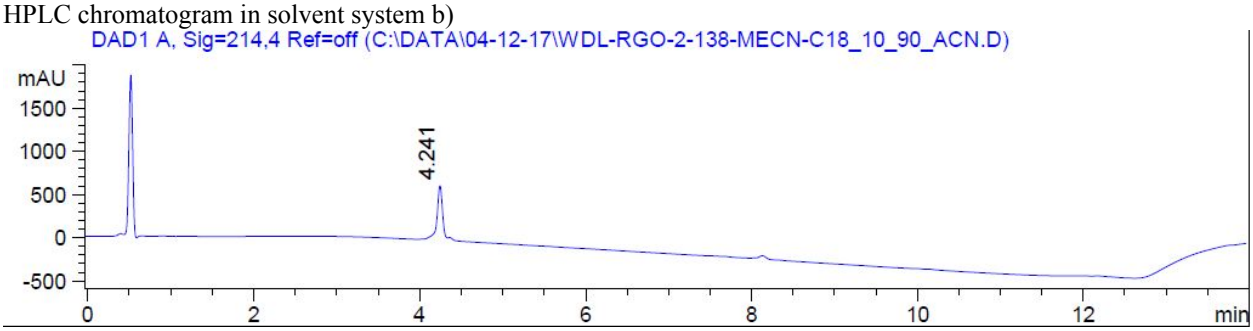

Ala-cyclo(Pra-D-Trp-Ala-Trp-D-Phe-Lys(allyl)), *S*-8

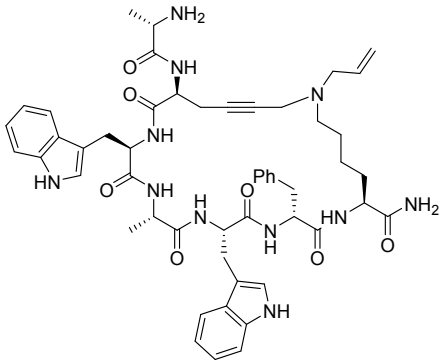

S-**8**: Heptapeptide resin **6b** (~300 mg, 0.09 mmol) was swollen in DMSO (5 mL) for 30 min in a syringe tube equipped with Teflon™ filter, and stopper, treated with CuI (3.0 mg, 0.02 mmol) and aqueous formaldehyde (50 µL, 0.69 mmol, 37% in H_2O), shaken on an automated shaker for 29 h, and filtered. After filtration, the resin was washed sequentially with AcOH/H_2O/DMF (5:15:80, v/v/v, ×3), DMF (×3), THF (×3), MeOH (×3), and DCM (×3). Examination by LCMS of a cleaved resin sample (5 mg) showed complete conversion, and a peak with molecular ion consistent with cyclic heptapeptide *S*-**8** was observed: MS *m/z*: calcd for $C_{52}H_{64}N_{11}O_7^+$ $[M+H]^+$ 954.5, found 954.5.

Resin-bound cyclic peptide *S*-**8** was deprotected and cleaved from the support using a freshly made solution of TFA/H_2O/TES (95:2.5:2.5, v/v/v, 5 mL) at rt for 2 h. The resin was filtered and rinsed with TFA (5 mL). The filtrate and rinses were concentrated until a crude oil persisted, from which a precipitate was obtained by addition of cold ether (10 mL). After centrifugation (1200 rpm for 10 min), the supernatant was removed, and the crude peptide precipitate was taken up in aqueous MeOH (10% v/v) and freeze-dried prior to purification. The resulting light brown fluffy material was purified by preparative HPLC to give cyclic heptapeptide *S*-**8** (1.5 mg, 2%) as a white fluffy material.

LCMS analysis of cyclic peptide *S*-**8** was performed using a linear gradient of a) 10–90% of MeOH containing 0.1% formic acid in H_2O (0.1% formic acid) over 10 min, then at 90% MeOH (0.1% formic acid) for 5 min, R_t = 6.32 min; b) 10–90% MeCN containing 0.1% formic acid in H_2O containing 0.1% formic acid over 10 min, then at 90% MeCN (0.1% formic acid) for 5 min, R_t = 4.47 min; HRMS *m/z*: calcd for $C_{52}H_{64}N_{11}O_7^+$ $[M+H]^+$ 954.4985, found 954.4973.

HPLC chromatogram in solvent system a)

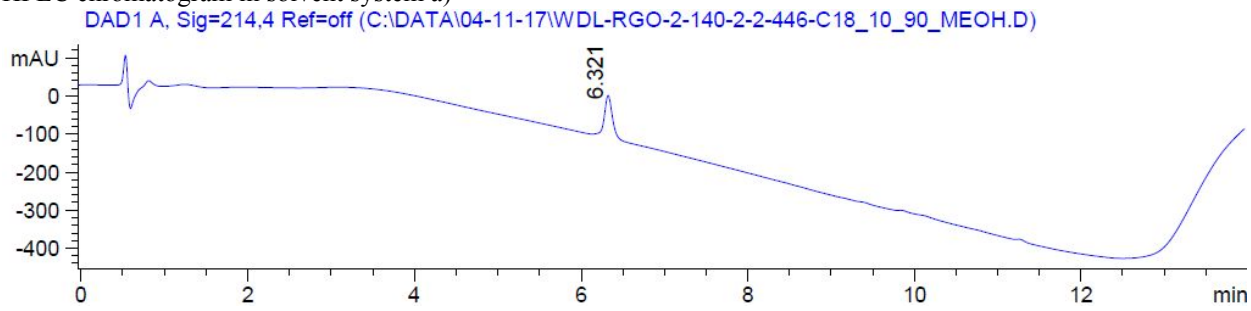

HPLC chromatogram in solvent system b)

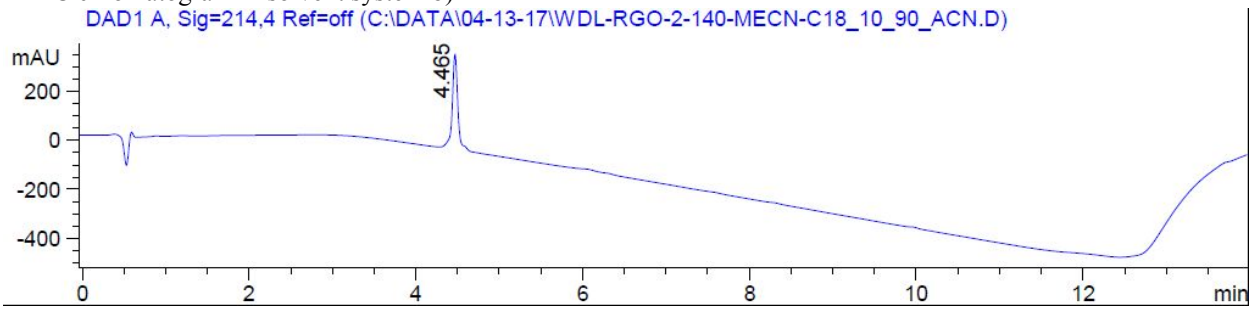

Ala-cyclo(D-Pra-Ala-Trp-D-Phe-Lys(allyl)), *R*-9

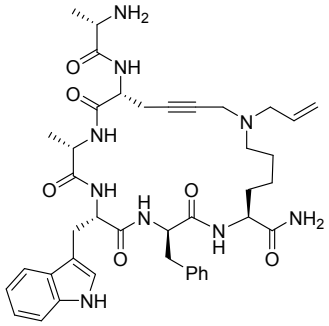

R-**9**: Hexapeptide resin **6c** (~600 mg, 0.156 mmol) was swollen in DMSO (6 mL) for 30 min in a syringe tube equipped with Teflon™ filter, and stopper, treated with CuI (5.0 mg, 0.03 mmol) and aqueous formaldehyde (70 µL, 0.94 mmol, 37% in H_2O), shaken on an automated shaker for 30 h, and filtered. After filtration, the resin was washed sequentially with AcOH/H_2O/DMF (5:15:80, v/v/v, ×3), DMF (×3), THF (×3), MeOH (×3), and DCM (×3). Examination by LCMS of a cleaved resin sample (5 mg) showed complete conversion, and a peak with molecular ion consistent with cyclic hexapeptide *R*-**9** was observed: MS *m/z*: calcd for $C_{41}H_{54}N_9O_6^+$ $[M+H]^+$ 768.4, found 768.4.

Resin-bound cyclic peptide *R*-**9** was deprotected and cleaved from the support using a freshly made solution of TFA/H_2O/TES (95:2.5:2.5, v/v/v, 5 mL) at rt for 2 h. The resin was filtered and rinsed with TFA (5 mL). The filtrate and rinses were concentrated until a crude oil persisted, from which a precipitate was obtained by addition of cold ether (10 mL). After centrifugation (1200 rpm for 10 min), the supernatant was removed and the crude peptide precipitate was taken up in aqueous MeOH (10% v/v) and freeze-dried prior to purification. The resulting light brown fluffy material was purified by preparative HPLC to give cyclic pentapeptide *R*-**9** (2.0 mg, 2%) as white fluffy material.

LCMS analysis of cyclic peptide *R*-**9** was performed using a linear gradient of a) 10–90% of MeOH containing 0.1% formic acid in H_2O (0.1% formic acid) over 10 min, then at 90% MeOH (0.1% formic acid) for 5 min, R_t = 5.62 min; b) 10–90% MeCN containing 0.1% formic acid in H_2O containing 0.1% formic acid over 10 min, then at 90% MeCN (0.1% formic acid) for 5 min, R_t = 3.96 min; HRMS *m/z*: calcd for $C_{41}H_{54}N_9O_6^+$ $[M+H]^+$ 768.4192, found 768.4176.

HPLC chromatogram in solvent system a)

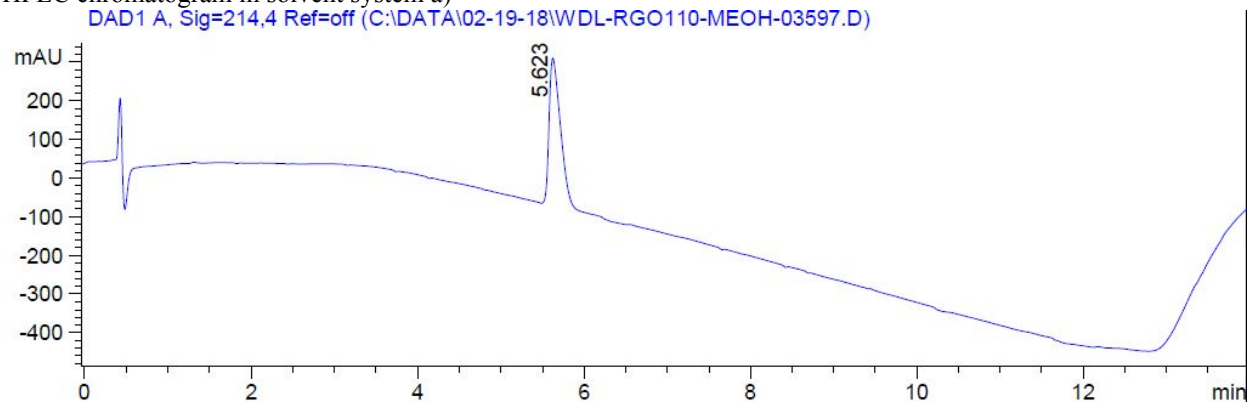

HPLC chromatogram in solvent system b)

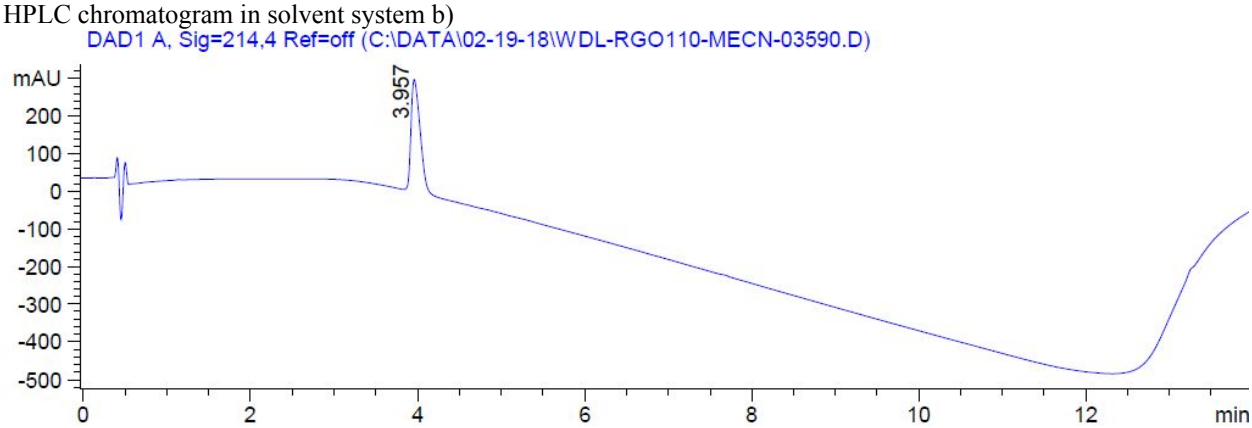

Ala-cyclo(Pra-Ala-Trp-D-Phe-Lys(allyl)), *S*-9

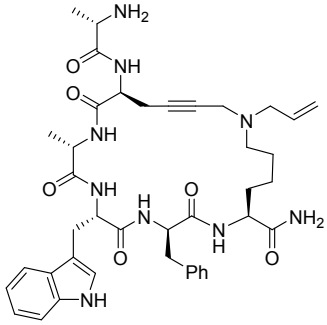

S-**9**: Hexapeptide resin **6d** (~600 mg, 0.14 mmol) was swollen in DMSO (6 mL) for 30 min in a syringe tube equipped with Teflon™ filter, and stopper, treated with CuI (5.0 mg, 0.03 mmol) and aqueous formaldehyde (60 µL, 0.84 mmol, 37% in H_2O), shaken on an automated shaker for 30 h, and filtered. After filtration, the resin was washed sequentially with AcOH/H_2O/DMF (5:15:80, v/v/v, ×3), DMF (×3), THF (×3), MeOH (×3), and DCM (×3). Examination by LCMS of a cleaved resin sample (5 mg) showed complete conversion, and a peak with molecular ion consistent with cyclic hexapeptide *S*-**9** was observed: MS *m/z*: calcd for $C_{41}H_{54}N_9O_6^+$ $[M+H]^+$ 768.4, found 768.4.

Resin-bound cyclic peptide *S*-**9** was deprotected and cleaved from the support using a freshly made solution of TFA/H_2O/TES (95:2.5:2.5, v/v/v, 5 mL) at rt for 2 h. The resin was filtered and rinsed with TFA (5 mL). The filtrate and rinses were concentrated until a crude oil persisted, from which a precipitate was obtained by addition of cold ether (10 mL). After centrifugation (1200 rpm for 10 min), the supernatant was removed and the crude peptide precipitate was taken up in aqueous MeOH (10% v/v) and freeze-dried prior to purification. The resulting light brown fluffy material was purified by preparative HPLC to give cyclic hexapeptide *S*-**9** (2.9 mg, 3%) as white fluffy material.

LCMS analysis of cyclic peptide *S*-**9** was performed using a linear gradient of a) 10–90% of MeOH containing 0.1% formic acid in H_2O (0.1% formic acid) over 10 min, then at 90% MeOH (0.1% formic acid) for 5 min, R_t = 4.80 min; b) 10–90% MeCN containing 0.1% formic acid in H_2O containing 0.1% formic acid over 10 min, then at 90% MeCN (0.1% formic acid) for 5 min, R_t = 4.30 min; HRMS *m/z*: calcd for $C_{41}H_{54}N_9O_6^+$ $[M+H]^+$ 768.4192, found 768.4172.

HPLC chromatogram in solvent system a)

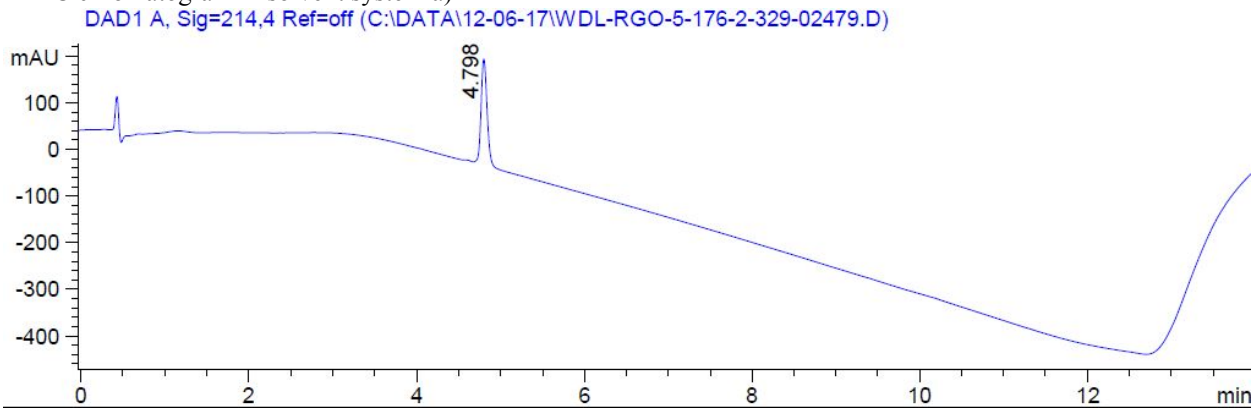

HPLC chromatogram in solvent system b)

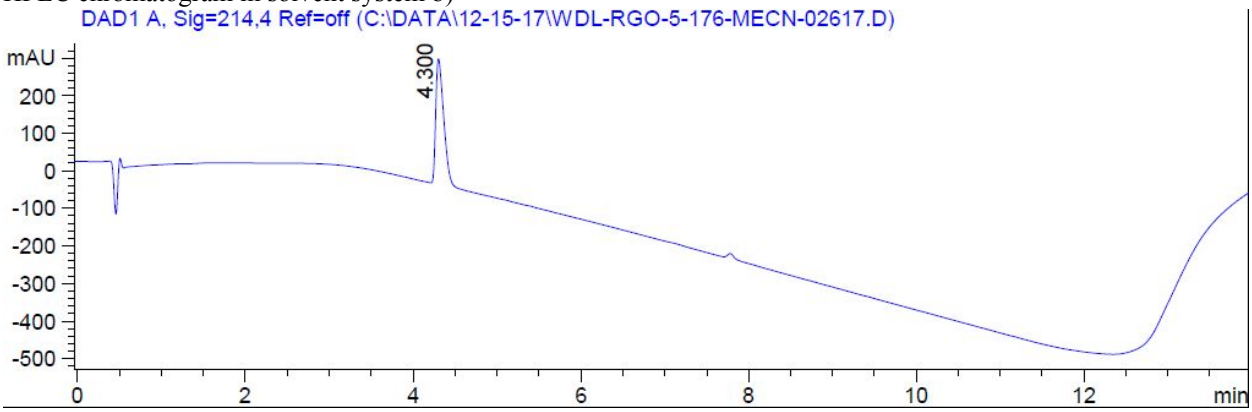

Fmoc-Lys(*o*-NBS)-OH, RGO5

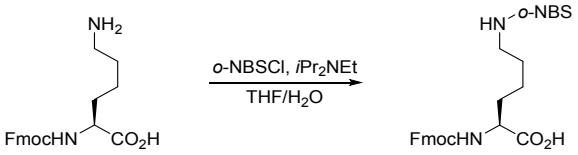

RGO5: Fmoc-Lys-OH (5.11 g, 10.9 mmol) was dissolved in THF/H_2O (1:1, 200 mL) and *i*Pr_2NEt (19 mL, 109 mmol) was added. *o*-NBSCl (2.68 g, 12.1 mmol) was then added in one portion and the reaction was stirred at room temperature. After 4 hours, the reaction was diluted with EtOAc (100 Ml) and washed with aqueous citric acid (100 mL × 3), water (100 mL) and brine (100 mL). The organic layer was then dried over $MgSO_4$ and the volatiles were removed by rotary evaporation to give **RGO5** (5.46 g, 90%) as a yellow oil. The amino acid was used without further purification.

^{1}H NMR (300 MHz, $CDCl_3$) δ ^{1}H NMR (300 MHz, $CDCl_3$) δ 8.13 – 8.07 (m, 1H), 7.83 – 7.79 (m, 1H), 7.76 (d, *J* = 7.5 Hz, 2H), 7.71 – 7.66 (m, 2H), 7.60 (d, *J* = 7.3 Hz, 2H), 7.39 (t, *J* = 7.4 Hz, 2H), 7.34 – 7.26 (m, 2H), 5.55 (dd, *J* = 14.2, 7.1 Hz, 2H), 4.84 (s, 1H), 4.40 (d, *J* = 6.9 Hz, 2H), 4.21 (t, *J* = 6.7, 1H), 3.15 – 3.02 (m, 2H), 1.85 (d, *J* = 5.6 Hz, 1H), 1.68 (dd, *J* = 14.2, 6.9 Hz, 1H), 1.63 – 1.50 (m, 2H), 1.49 – 1.36 (m, 3H). ^{13}C NMR (75 MHz, $CDCl_3$) δ 176.2, 171.5, 156.4, 148.1, 143.9, 141.4, 133.7, 132.9, 131.1, 127.9, 127.2, 125.5, 125.2, 120.1, 67.4, 60.7,

53.5, 50.8, 47.2, 43.4, 31.8, 29.0, 22.06, 21.2, 14.3. ESI-MS *m/z*: calcd for $C_{27}H_{28}N_3O_8S^+$ $[M+H]^+$ 554.2, found 554.3.

NMR Analysis

Numbering

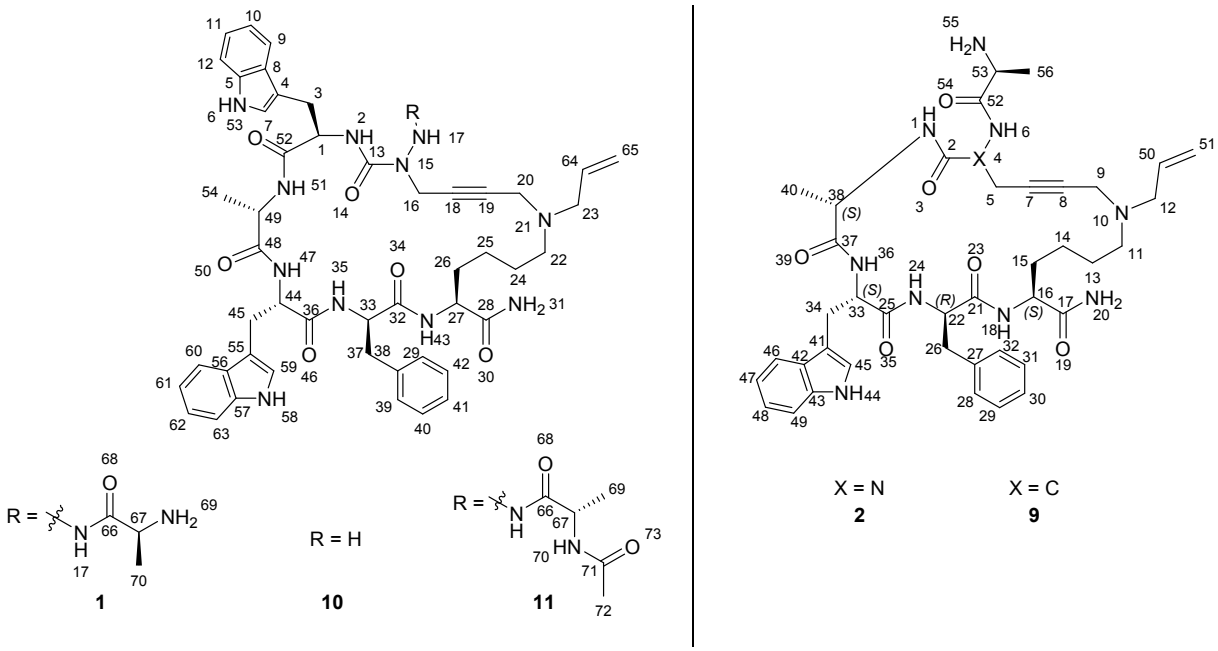

Figure S1. Proton assignments in D_2O were derived from TOCSY, NOESY, COSY, HSQC and HMBC spectra recorded at 25 °C on a 900 MHz BRUKER Avance III HD NMR spectrometer equipped with a TCI cryoprobe. NOE build-ups were recorded without solvent suppression with mixing times of 100, 200, 300, 400, 500, 600 and 700 ms. The relaxation delay was set to 2.5 s, and 16 scans were recorded with 16384 points in the direct dimension and 512 points in the indirect dimension. Distances were calculated using geminal methylene protons (1.78 Å) as reference. Comparable distances obtained from various methylene proton pairs within the peptides served as a measure of the data quality. The NOE peak intensities were calculated using normalization of both cross peaks and diagonal peaks according to ([cross peak1 × cross peak2]/[diagonal peak1 × diagonal peak2])$^{0.5}$. At least 4 mixing times giving a linear (r2 > 0.95, typically > 0.98) initial NOE rate for every distance were used to determine σ_{ij} build-up rates. Distances were determined according to the equation $r_{ij}=r_{ref}(\sigma_{ref}/\sigma_{ij})^{(1/6)}$, where r_{ij} is the distance between protons i and j in Ångström, r_{ref} is 1.78 Å and σ_{ref} and σ_{ij} is the build-up for the reference and the i–j proton pair, respectively.

Table S1. ^{1}HNMR assignment (ppm) in D_2O for **1**, **10** and **11**.

Proton No.	**1**	**10**	**11**
1	4.32	4.73	4.32
3	3.27; 3.22	3.42	3.30; 3.17
16	4.80; 4.06	4.01; 3.98	4.81; 3.94
20	3.87; 3.77	3.09	3.96
22	2.88; 2.82	4.14	3.05
23	3.56	3.86	3.7
24	1.55	1.59	1.59
25	1.29; 1.00	1.17; 1.04	1.32; 1.05
26	1.81; 1.64	1.73; 1.63	1.82; 1.62
27	4.26	4.3	4.27
33	4.43	4.56	4.41
37	2.84; 2.79	2.93; 2.82	2.86; 2.71
44	4.35	4.5	4.28
45	3.14	3.18	3.15
49	3.95	4.17	4.11
54	0.94	1.18	0.96
64	5.83	5.98	5.84
65	5.52	5.75	5.59
67	3.97	–	4.11
69	–	–	1.21
70	1.48	–	–
72	–	–	1.98

Table S2. ^{1}HNMR assignment (ppm) in D_2O for **2** and *S*-**9**.

Proton No.	**2**	*S*-**9**
4	–	4.41
5	4.65; 4.06	2.78; 2.70
9	3.84	3.67
11	2.97	2.87
12	3.56	3.47
13	1.57	1.57
14	1.38; 1.17	1.34; 1.23
15	1.81; 1.72	1.80; 1.73
16	4.32	4.22
22	4.50	4.36
26	2.78	2.68; 2.58
33	4.59	4.48
34	3.14	3.15; 3.07
38	4.13	4.32
40	1.20	1.35
50	5.88	5.84
51	5.49	5.44
53	4.05	4.02
56	1.51	1.46

Table S3. Interproton distances (Å) for **1** derived from NOE build-up measurements in D_2O.

No.	**Proton i**	**Proton j**	**σ**	**r2**	**Distance r_{ij} (Å)**
1	33	27	3.8E-06	0.99	3.79
2	33	25A	2.6E-06	0.99	4.04
3	33	20A	4E-07	0.99	5.52
4	33	24	1.7E-06	0.97	4.34
5	33	26B	1.9E-06	0.99	4.26
6	33	16B	0.000002	0.97	4.22
7	44	37A	1.01E-05	0.98	3.22
8	27	24	4.16E-05	0.98	2.55
9	27	25A	1.24E-05	0.99	3.11
10	27	23	2.4E-06	0.99	4.09
11	27	20B	2.9E-06	0.98	3.97
12	33	44	6.4E-06	0.96	3.48
13	33	45	5.6E-06	0.96	3.56
14	64	24	1.9E-06	0.95	4.26
15	64	20B	4.4E-06	0.99	3.70
Ref	26A	26B	0.000356	0.99	1.78

Table S4. Interproton distances (Å) for **10** derived from NOE build-up measurements in D_2O.

No.	Proton i	Proton j	σ	r2	Distance r_{ij} (Å)
1	33	20	0.0000016	0.97	4.83
2	33	45	0.0000067	0.98	3.80
3	44	25A	0.0000031	0.99	4.32
4	27	24	0.0000196	0.98	3.18
5	27	45	0.0000024	0.97	4.51
6	27	37A	0.0000021	0.97	4.61
7	27	20	0.0000047	0.99	4.03
8	27	25A	0.000005	0.99	4.03
9	27	3	0.0000009	0.99	5.31
10	49	45	0.000005	0.97	3.99
11	49	37A	0.0000008	0.98	5.42
12	49	3	0.0000086	0.99	3.65
13	64	27	0.000001	0.98	5.22
14	64	24	0.0000008	0.97	5.42
15	64	20	0.000004	0.97	4.14
16	64	22	0.0000075	0.99	3.73
Ref.	37A	37B	0.0006363	0.99	1.78

Table S5. Interproton distances (Å) for **11** derived from NOE build-up measurements in D_2O.

No.	Proton i	Proton j	σ	r2	Distance r_{ij} (Å)
1	33	20	6E-07	0.97	5.89
2	33	26B	2.2E-06	0.99	4.74
3	33	25A	1.9E-06	0.97	4.86
4	33	45	8.8E-06	0.99	3.77
5	44	37B	5.17E-05	0.98	2.80
6	27	25B	1.36E-05	0.99	3.50
7	27	23	2.1E-06	0.98	4.78
8	27	22	2.04E-05	0.99	3.27
9	27	26A	0.000153	0.99	2.34
10	64	22	2.81E-05	0.99	3.10
11	64	26B	3.4E-06	0.99	4.41
12	64	20	1.12E-05	0.99	3.62
Ref.	26A	26B	0.000789	0.99	1.78

Table S6. Interproton distances (Å) for **2** derived from NOE build-up measurements in D_2O.

No.	Proton i	Proton j	σ	r2	Distance r_{ij} (Å)
1	15A	16	0.0000233	0.97	2.58
2	11	16	0.0000023	0.97	3.79
3	13B	16	0.0000041	0.99	3.45
4	14B	16	0.0000019	0.98	3.92
5	15A	38	0.0000006	0.98	4.75
6	40	33	0.0000011	0.98	4.29
7	11	9	0.0000103	0.99	2.96
8	14B	9	0.0000008	0.99	4.52
9	13B	9	0.0000074	0.99	3.12
10	12	9	0.0000065	0.97	3.19
11	14A	12	0.0000014	0.99	4.12
12	11	12	0.0000091	0.98	3.02
13	14B	11	0.0000089	0.99	3.03
14	15A	11	0.0000026	0.98	3.72
15	14A	26	0.0000005	0.98	4.89
16	14B	15A	0.0000071	0.98	3.14
17	13B	15A	0.0000031	0.96	3.61
18	14B	13B	0.0000054	0.98	3.29
19	26	51	0.0000004	0.96	5.08
Ref.	5A	5B	0.0002158	0.99	1.78

Table S7. Interproton distances (Å) for *S*-**9** derived from NOE build-up measurements in D_2O.

No.	Proton i	Proton j	σ	r2	Distance r_{ij} (Å)
1	50	9	0.00000280	0.96	3.81
2	33	26B	0.00000059	0.99	4.95
3	4	5A	0.00005397	0.99	2.33
4	22	14A	0.00000063	0.99	4.89
5	22	34B	0.00000088	0.99	4.63
6	38	13	0.00000061	0.97	4.92
7	16	14B	0.00001519	0.99	2.88
8	16	15B	0.00001829	0.96	2.79
9	16	13	0.00001018	0.99	3.08
10	16	11	0.00000223	0.97	3.96
11	9	14B	0.00000225	0.98	3.96
12	9	12	0.00000937	0.98	3.12
13	9	11	0.00000976	0.98	3.10
14	9	13	0.00001816	0.99	2.79
15	12	11	0.00001355	0.99	2.93
16	12	13	0.00000712	0.99	3.27
17	11	15A	0.00000456	0.99	3.52
18	11	13	0.00001505	0.99	2.88
19	11	14B	0.00001659	0.99	2.84
20	13	14B	0.00000736	0.95	3.25
Ref.	34A	34B	0.00027125	0.98	1.78

Monte Carlo Molecular Mechanics (MCMM) conformational search

In order to provide ensembles covering the available conformational space of the cyclic peptides, careful Monte Carlo conformational analyses were performed using the OPLS and the Amber* force fields using the GB/SA water continuum solvent model.[2] These conformational searches were performed using the Monte Carlo algorithm with intermediate torsion sampling, 50000 Monte Carlo steps, and a RMSD cut-off set to 2.0 Å, followed by Molecular Mechanics energy minimization, with the software Macromodel (v.9.1) as implemented in the Schrödinger package. The energy minimization was performed using the Polak-Ribiere type conjugate gradient (PRCG) with maximum iteration steps set to 5000. The number of torsion angles allowed to vary during each Monte Carlo step ranged from 1 to n - 1 where n equals the total number of rotatable bonds. Amide bonds were fixed in the trans configuration. All conformations within 42 kJ/mol from the global minimum were saved. The results of the independent searches performed using OPLS-2005 or Amber* as force field, are given below. The ensembles from the conformational searches were combined and elimination of redundant conformations by comparisons of the heavy atom coordinates applying the RMSD cutoff 2.0 Å was performed, giving the ensembles used for NAMFIS (NMR Analysis of Molecular Flexibility in Solution). The conformational searches fulfilled the equation $1-(1-(1/N))^M$ as an estimate of the probability that the conformational search is complete, where N is the total number of conformers and M is the number of search steps.[3] Moreover, the seven 'lowest energy' conformations were found at least 7 times each on average, which is also an indicator of search completeness.[4]

Table S8. Result of the MCMM conformational analysis.

Peptide	Force Field	Total number of unique conformations found	Following redundant conformer elimination[a]
1	OPLS	312	129
	Amber*	176	
2	OPLS	54	37
	Amber*	17	
S-**9**	OPLS	22	60
	Amber*	35	
10	OPLS	467	171
	Amber*	132	
11	OPLS	373	165
	Amber*	266	

[a]Conformations obtained after redundant conformation elimination with the root-mean-square deviation cutoff 2.0 Å for heavy atoms. These ensembles were used as input in the NAMFIS analysis.

NAMFIS analysis

Solution ensembles were determined by fitting the experimentally measured distances to those back-calculated for computationally predicted conformations following previously described protocols.[5] CH_2-signals were treated according to the equation $d=(((d_1^{-6})+(d_2^{-6}))/2)^{-1/6}$, and methyl signals according to $d=(((d_1^{-6})+(d_2^{-6})+(d_3^{-6}))/3)^{-1/6}$. The NAMFIS ensemble analyses were validated using standard methods, that is, through evaluation of the reliability of the conformational restraints by the addition of 10% random noise to the experimental data, by the random removal of individual restraints, and by comparison of the experimentally observed and back-calculated distances.

Table S9. Result of the NAMFIS-analyses for the azapeptides **1**, **10** and **11** in D_2O.

Conf. No.	Population (%) in ensemble[a]	IMHB[b]	Similar conf. within ensemble	Similar conf. in the other ensembles	Conformational group
1					
1	3	3	2	7, 16	A
2	28	4	1	7, 16	A
3	11	2	4, 5, 6	13, 15, 17	B
4	8	3	3, 5, 6	13, 15, 17	B
5	11	1	3, 4, 6	13, 15, 17	B
6	36	3	3, 4, 5	13, 15, 17	B
10					
7	2	4	unique	1, 2, 16	A
8	7	-	9, 11	unique	C
9	11	-	8, 11	unique	C
10	2	3	unique	21	D
11	3	-	8, 9	unique	C
12	25	-	unique	unique	-
13	8	-	15	3-6, 17	B
14	6	4	unique	unique	-
15	33	2	13	3-6, 17	B
11					
16	22	3	unique	1, 2, 7	A
17	8	2	unique	3-6, 13, 15	B
18	22	3	unique	unique	-
19	8	3	unique	unique	-
20	16	5	unique	unique	-
21	21	4	unique	10	D

[a]Population of the indicated conformer in solution. [b]Intramolecular hydrogen bonds.

Table S10. Result of the NAMFIS-analyses for **2** and *S*-**9** in D_2O.

Conf. No.	Population (%) in ensemble[a]	IMHB[b]	Similar conf. within ensemble	Similar conf. in the other ensemble
2				
22	57	4	-	2
23	11	3	-	-
24	1	3	11	3
25	20	3	10	3
26	11	2	-	-
S-**9**				
27	16	4	-	-
28	11	2	-	8
29	5	1	7	10,11
30	39	2	6	-
31	27	1	-	-

[a]Population of the indicated conformer in solution. [b]Intramolecular hydrogen bonds.

Table S11. Experimentally determined and back-calculated (NAMFIS) interproton distances (Å).

1		**10**		**11**		**2**		***S*-9**	
Exp.	Calc.	Exp.	Calc.	Exp.	Calc.	Exp.	Calc.	Exp.	Calc.
3.79	4.48	4.83	4.93	5.89	5.77	2.58	2.46	3.81	3.77
4.04	4.44	3.80	5.04	4.74	4.83	3.79	5.40	4.95	5.18
5.52	5.62	4.32	4.84	4.86	4.68	3.45	3.24	2.33	2.49
4.34	5.09	3.18	2.94	3.77	5.16	3.92	3.58	4.89	5.01
4.26	5.06	4.51	5.83	2.80	4.49	4.75	5.79	4.63	4.91
4.22	4.91	4.61	5.21	3.50	3.26	4.29	5.00	4.92	4.96
3.22	4.74	4.03	5.71	4.78	4.79	2.96	2.95	2.88	2.88
2.55	3.02	4.03	3.42	3.27	3.40	4.52	4.08	2.79	2.71
3.11	2.91	5.31	5.82	2.34	2.54	3.12	3.29	3.08	2.96
4.09	5.59	3.99	5.27	3.10	3.28	3.19	2.95	3.96	4.56
3.97	5.12	5.42	5.39	4.41	4.69	4.12	4.69	3.96	4.88
3.48	4.52	3.65	4.91	3.62	3.53	3.02	2.84	3.12	2.79
3.56	4.84	5.22	5.23			3.03	2.75	3.10	3.03
4.26	4.39	5.42	4.59			3.72	4.59	2.79	2.86
3.70	3.31	4.14	3.44			4.89	4.75	2.93	2.81
		3.73	3.68			3.14	2.65	3.27	3.34
						3.61	2.76	3.52	3.37
						3.29	2.68	2.88	2.62
						5.08	5.56	2.84	2.80
								3.25	2.60
RMSD = 0.87		RMSD = 0.86		RMSD = 0.65		RMSD = 0.62		RMSD = 0.32	

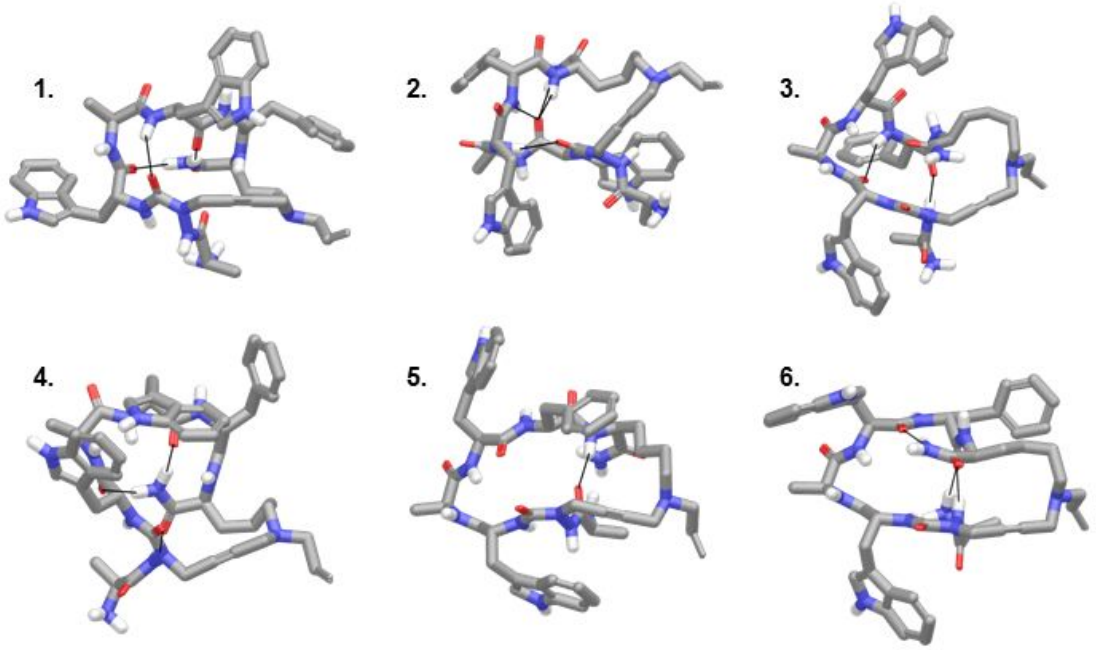

Figure S2. The solution conformations of **1** in D_2O as selected by the NAMFIS-analysis. Hydrogen bonds are indicated by black lines. Non-polar hydrogens are omitted for clarity.

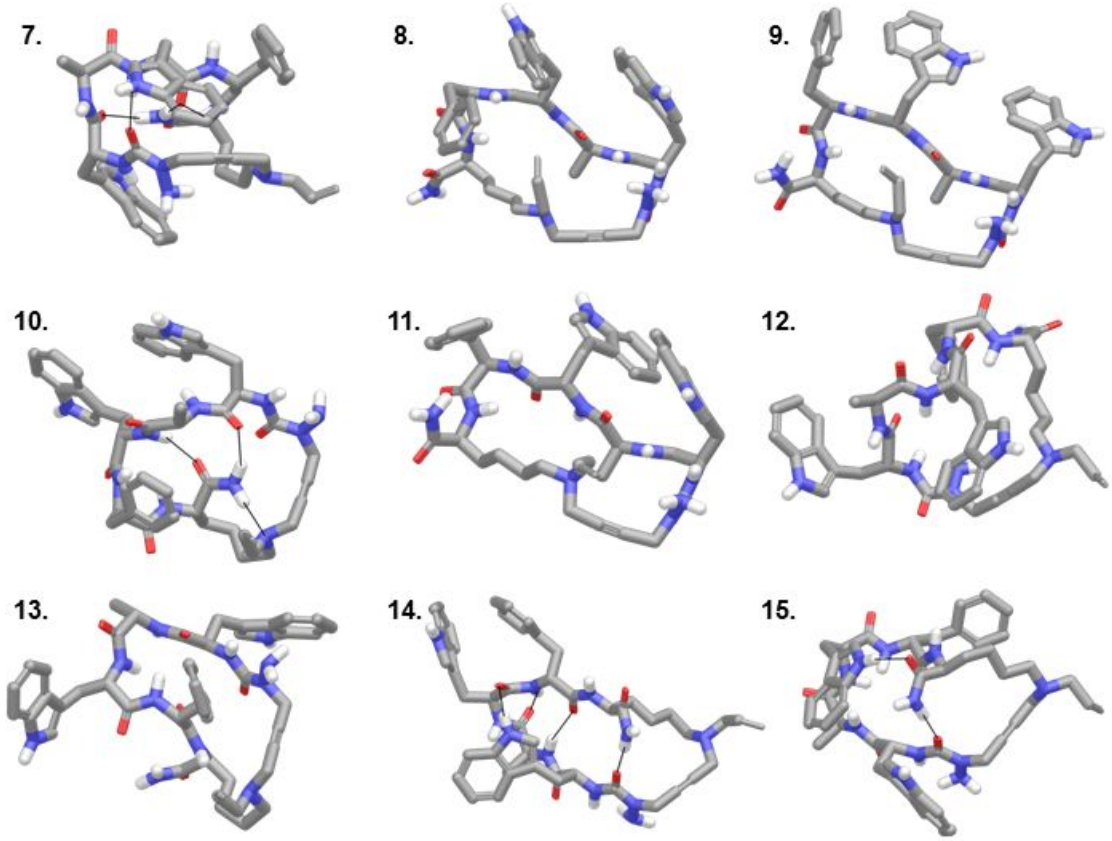

Figure S3. The solution conformations of **10** in D_2O as selected by the NAMFIS-analysis. Hydrogen bonds are indicated by black lines. Non-polar hydrogens are omitted for clarity.

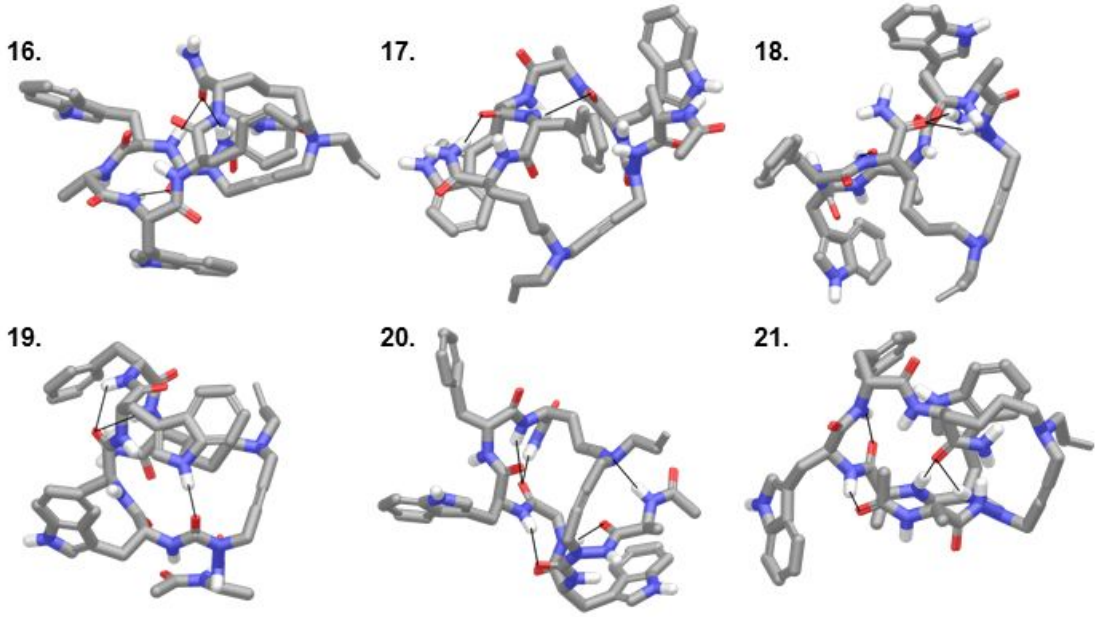

Figure S4. The solution conformations of **11** in D_2O as selected by the NAMFIS-analysis. Hydrogen bonds are indicated by black lines. Non-polar hydrogens are omitted for clarity.

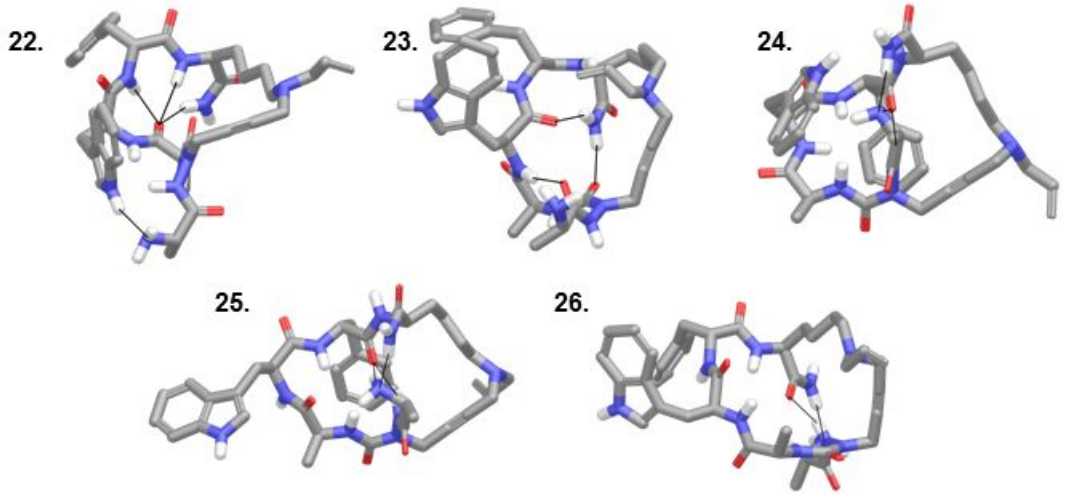

Figure S5. The solution conformations of **2** in D_2O as selected by the NAMFIS-analysis. Hydrogen bonds are indicated by black lines. Non-polar hydrogens are omitted for clarity.

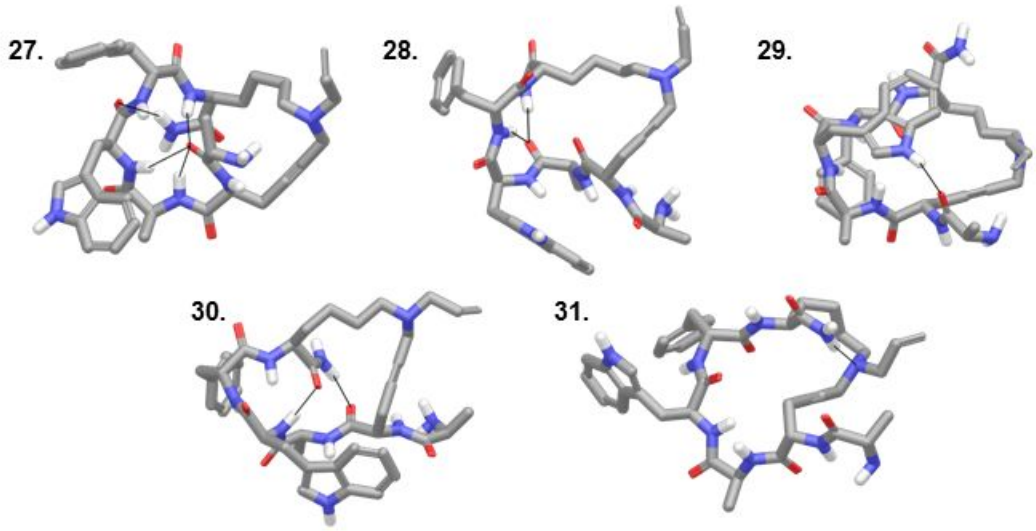

Figure S6. The solution conformations of *S*-**9** in D_2O as selected by the NAMFIS-analysis. Hydrogen bonds are indicated by black lines. Non-polar hydrogens are omitted for clarity.

Aza-nitrogen geometry

In addition to the description of the conformational ensembles using NAMFIS, as described above, we have evaluated the likelihood that the N-4 nitrogen would adopt sp2 or sp3 chirality using the Akaike information criterion (AIC),[6] which is the golden standard for model comparison and selection.[7] It allows selection of the model best reproducing reality, and the comparison of the quality of various models. Presuming random (Gaussian) errors, the maximum likelihood of parameters can be estimated by chi-squared minimization, where the chi-squared statistics is defined as

$$\chi^2 = \sum_{i=1}^{n} \frac{(R_{i.calc} - R_{i.exp})^2}{\sigma_i^2}$$

where R_i is the calculated and measured interatomic distances, and $\square_i$ is the experimental error, here expressed as the root-mean-square-deviation RMSD value, expressed as follows for all distances:

$$\mathrm{RMSD} = \sqrt{\frac{1}{N}\sum_{i=1}^{N} \delta_i^2}$$

Using the technique developed by Akaike, the model showing the lowest criterion value (AIC) is considered to best reproduce reality, here meaning the ensemble closest reflecting the properties of **2**, as described by

$$\mathrm{AIC} = \chi^2 + 2\mathrm{k}$$

where, k is the number of model-free parameters in the model, here the number of theoretical conformations selected by the NAMFIS algorithm.

The best model has the lowest AIC value, and thus the lowest relative distance to the 'truth', the real ensemble. The difference between different models' ability to describe truth is given by

$$\Delta_i\mathrm{AIC} = AIC_i - AIC_{min}$$

The likelihood of a model is estimated by the 'Akaike weight, w_i:

$$w_i = \frac{e^{-\frac{1}{2}\Delta AIC_i}}{\sum_r^R e^{-\frac{1}{2}\Delta AIC_r}}$$

which is the normalized relative likelihood of a model (weight of evidence), i.e. the denominator is here the relative likelihoods of all candidate models (R is the number of models, r the model being considered). The Akaike weight can be converted to Evidence Ratio (ERi), which expresses the relative likelihood in terms of evidence about a model being better in an information criteria sense.

$ER_i = \frac{w_{best}}{w_i}$ and $LER_i = \log_{10}(ER_i)$

where w_{best} is the weight of the best model, w_i the weight of other individual models, and LER_i the Logarithmic Evidence Ratio of a model.

In short, the best model has the lowest AIC value, the ERi of 1 (all other less likely models have a higher ERi) and a LERi value of 0. The difference in LERi expresses the evidence how much better the best proposed model is as compared to all other proposed models, where a LERi 0−0.5 is interpreted as 'weak', 0.5−1 as 'substantial', 1−2 as 'strong' and >2 as 'decisive'.[8] A summary of AIC results for **2** on the three ensembles are given in below. The conclusions drawn based on AIC analysis are in line with the alternative Bayesian information criterion analysis (BIC) that is an alternative method for model selection with the model having the lowest BIC being most likely to best describe reality.

Table S12. Result of the NAMFIS-analyses for azapeptide **2** using the ensemble of **2**, *S*-**9** and *R*-**9**.

Ensemble	**2**		*S*-**9**		*R*-**9**	
	Conf. No.	Population (%)	Conf. No.	Population (%)	Conf. No.	Population (%)
	22	57	32	3	40	23
	23	11	33	15	41	1
	24	1	28	2	42	24
	25	20	34	5	43	26
	26	11	35	3	44	1
			36	1	45	1
			37	39	46	1
			38	14	47	1
			39	19	48	1
					49	4
					50	3
					51	1
					52	1
					53	9
					54	1
					55	2
					56	1
Exp.[a]	Calc.[a]		Calc.[a]		Calc.[a]	
2.58	2.46		3.43		3.11	
3.79	5.40		5.20		3.98	
3.45	3.24		3.66		3.60	
3.92	3.58		3.72		4.26	
4.75	5.79		4.80		5.07	
4.29	5.00		5.01		5.25	
2.96	2.95		2.91		2.14	
4.52	4.08		4.99		3.38	
3.12	3.29		3.12		2.71	
3.19	2.95		2.83		3.11	
4.12	4.69		4.62		2.97	
3.02	2.84		2.78		2.12	
3.03	2.75		2.73		3.34	
3.72	4.59		3.43		4.01	
4.89	4.75		3.50		4.84	
3.14	2.65		2.57		2.16	
3.61	2.76		2.94		2.75	
3.29	2.68		2.62		2.14	
5.08	5.56		6.79		5.90	
RMSD[b]	0.62		0.73		0.71	

[a]Experimentally determined and back-calculated (NAMFIS) interproton distances (Å). [b]Root mean square deviation of experimental and calculated distances.

Table S13. Summary of the results of the Akaike Information Criterion analyses of the fit of the three theoretical ensembles to the experimental data of **2**.

	Input ensemble		
Statistical parameter[a]	**2**	***S*-9**	***R*-9**
χ^2	7.0	10.9	15.7
AIC	17.0	28.9	49.7
BIC	27.4	43.4	93.1
AICc	18.1	35.6	57.7
ΔAICc	0.00	11.9	32.7
w_i	1.00	0.0025458	0.0000001
ER_i	1.00	391.80	13109584.56
LER_i [a]	**0.0**	**2.6**	**7.1**

[a]Here, χ^2 is Pearson's statistical hypothesis test that determines whether there is a significant difference between expected and observed values, AIC is the Akaike information criterion, BIC the Bayesian information criterion, AICc is the small sample size corrected AIC that has a compensation for overfitting for systems with small sample size, ΔAICc is the difference in AIC of an individual model as compared to the best model, w_i is the Akaike weight of the individual models, i.e. the weight of evidence in favor of a model being the actual best model for a given data, ER_i is the evidence ratio describing the relative likelihood of a pair of models, representing the evidence about fitted models as to which is better in an information criteria sense, and LERi is the logarithmic evidence ratio. LERi = 0–0,5: minimal; 0,5–1: substantial; 1–2: strong; >2 decisive evidence.

Original NMR spectra

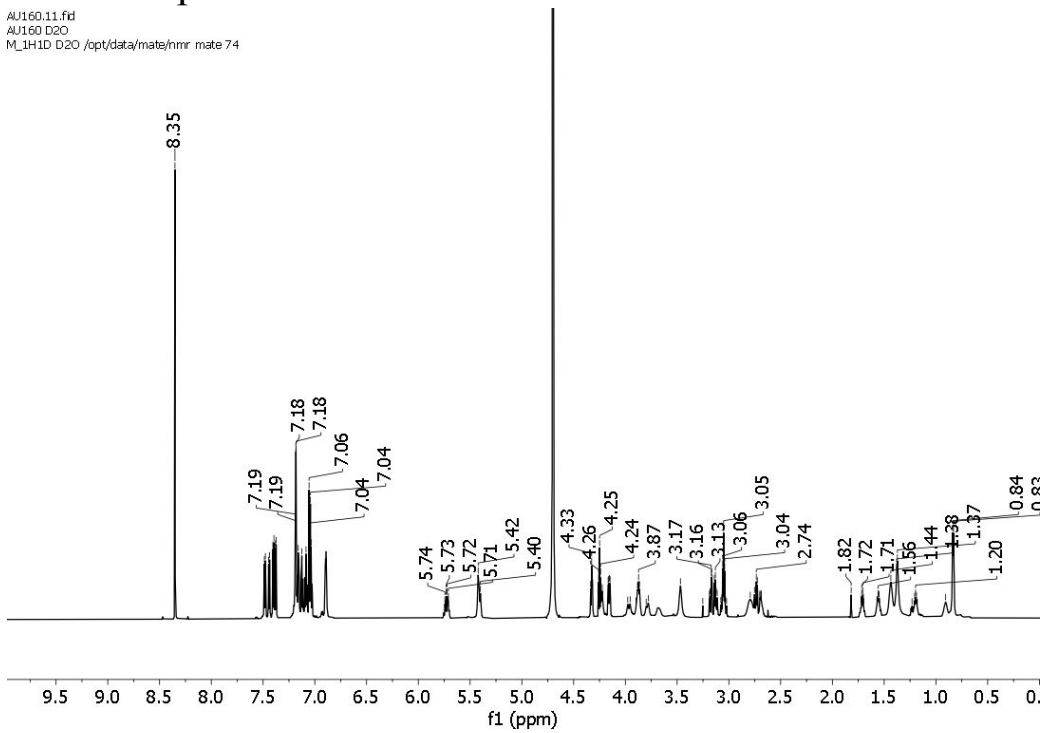

Figure S7. The ^{1}H NMR spectrum of compound **1** acquired at 800 MHz, 25 °C in D_2O.

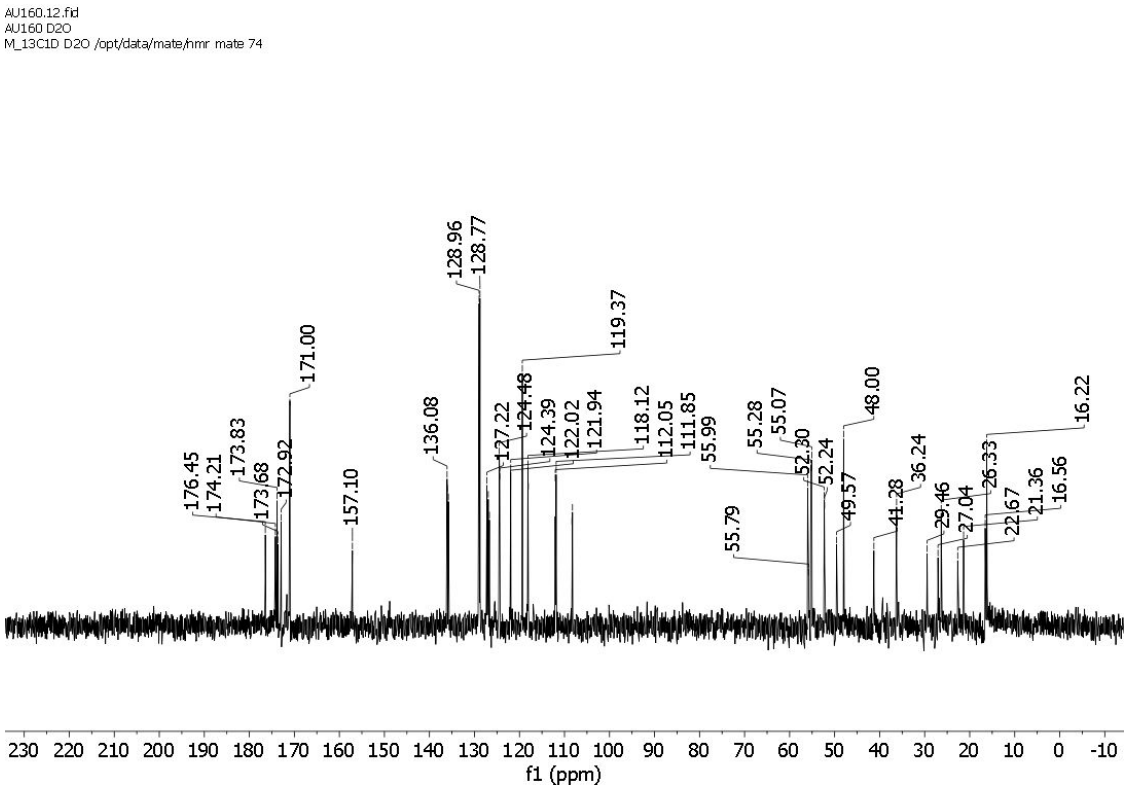

Figure S8. The ^{13}C NMR spectrum of compound **1** acquired at 200 MHz, 25 °C in D_2O.

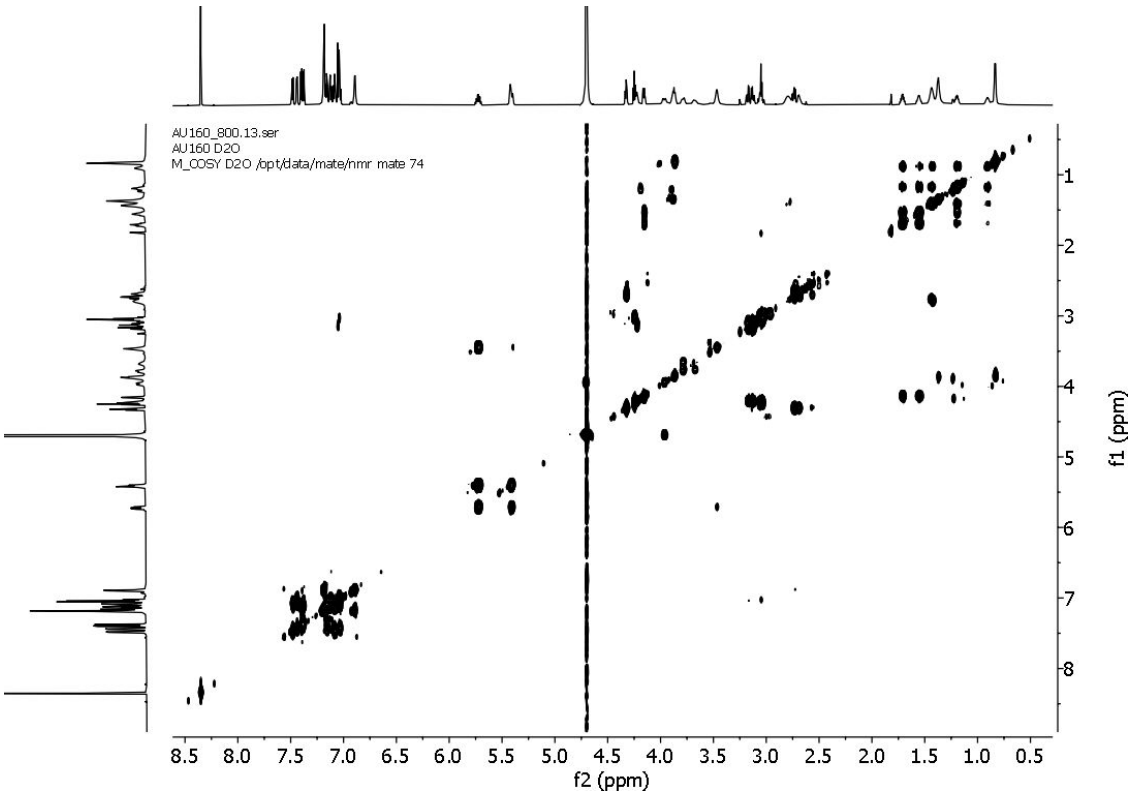

Figure S9. The COSY spectrum of compound **1** acquired at 800 MHz, 25 °C in D_2O.

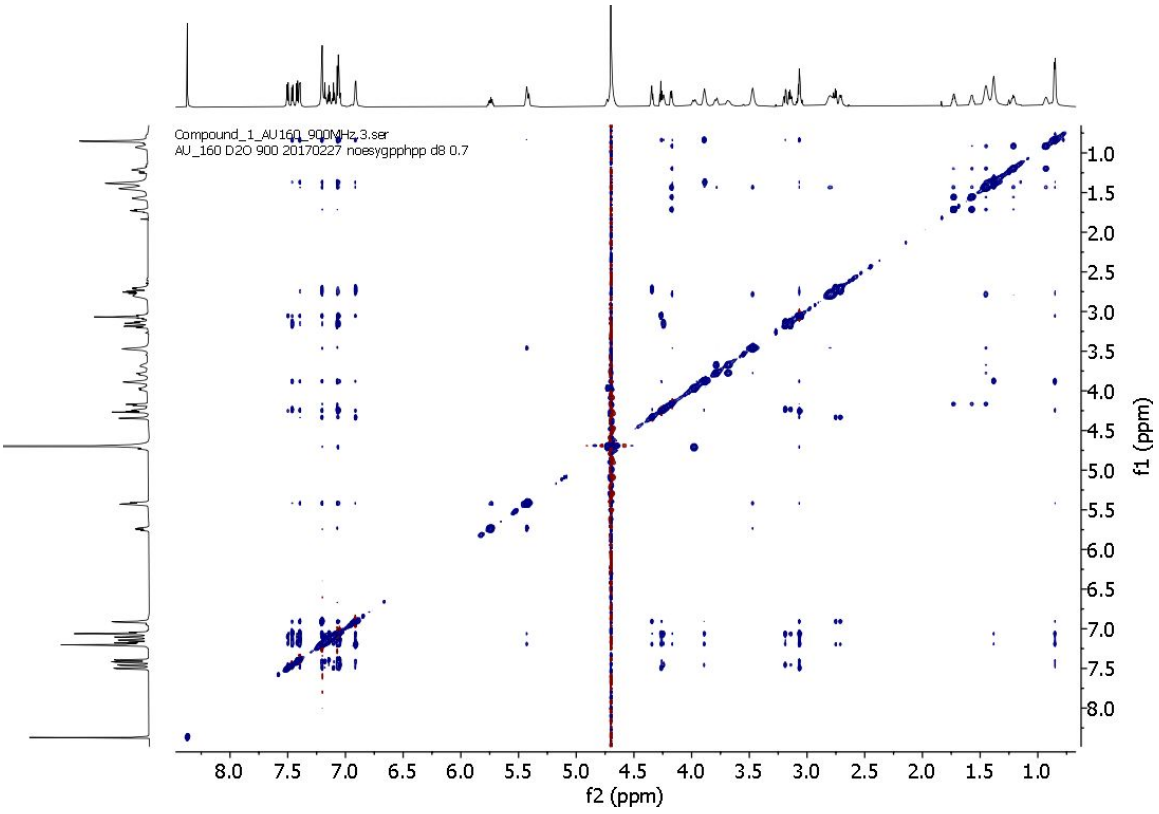

Figure S10. The NOESY spectrum of compound **1** acquired at 900 MHz, 25 °C in D_2O ,d_1=2.5 and mix =0.7 s.

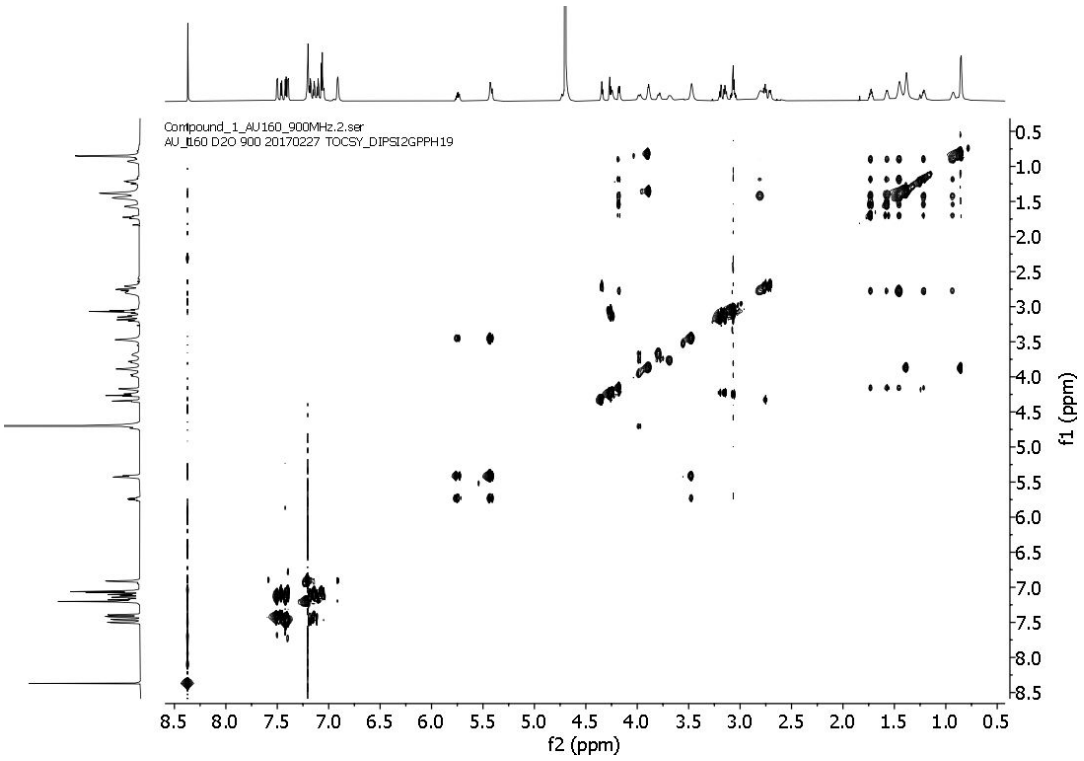

Figure S11. The TOCSY spectrum of compound **1** acquired at 900 MHz, 25 °C in D_2O.

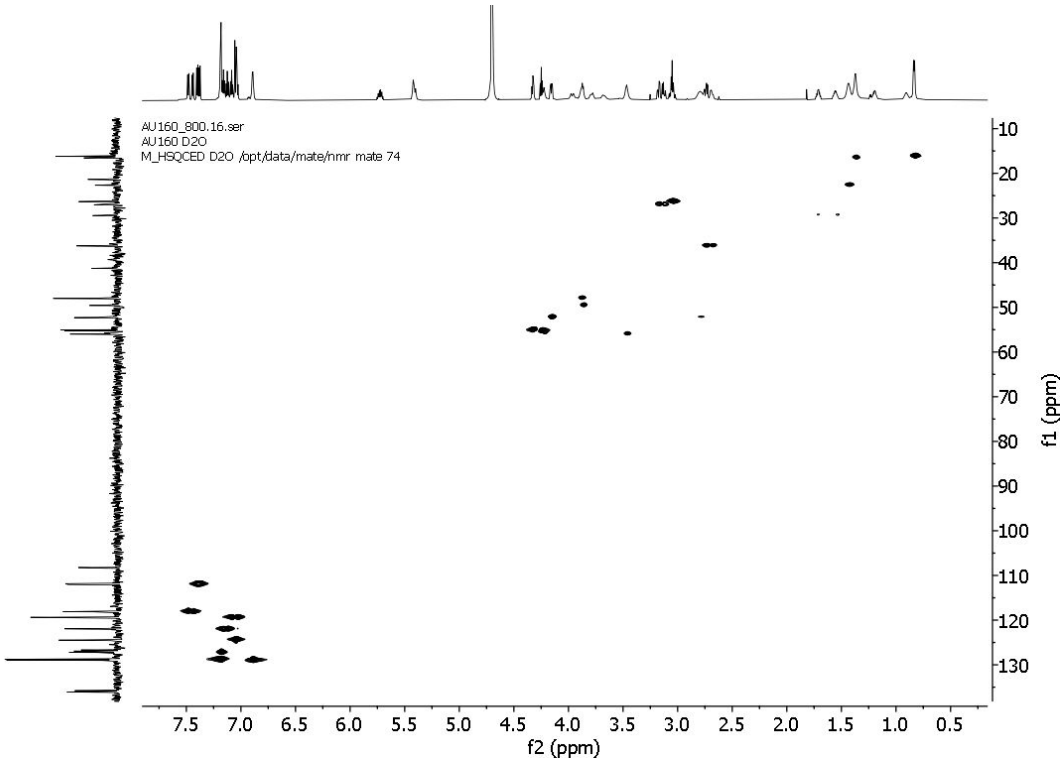

Figure S12. The HSQC spectrum of compound **1** acquired at 800/200 MHz, 25 °C in D_2O.

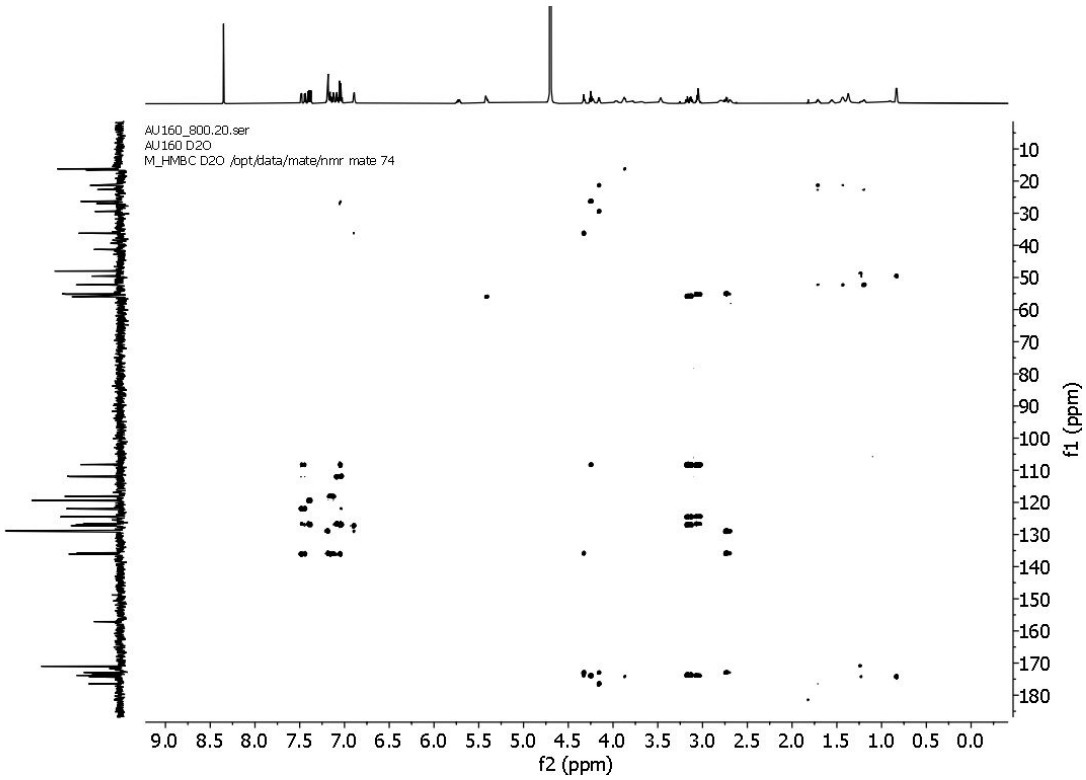

Figure S13. The HMBC spectrum of compound **1** acquired at 800/200 MHz, 25 °C in D_2O.

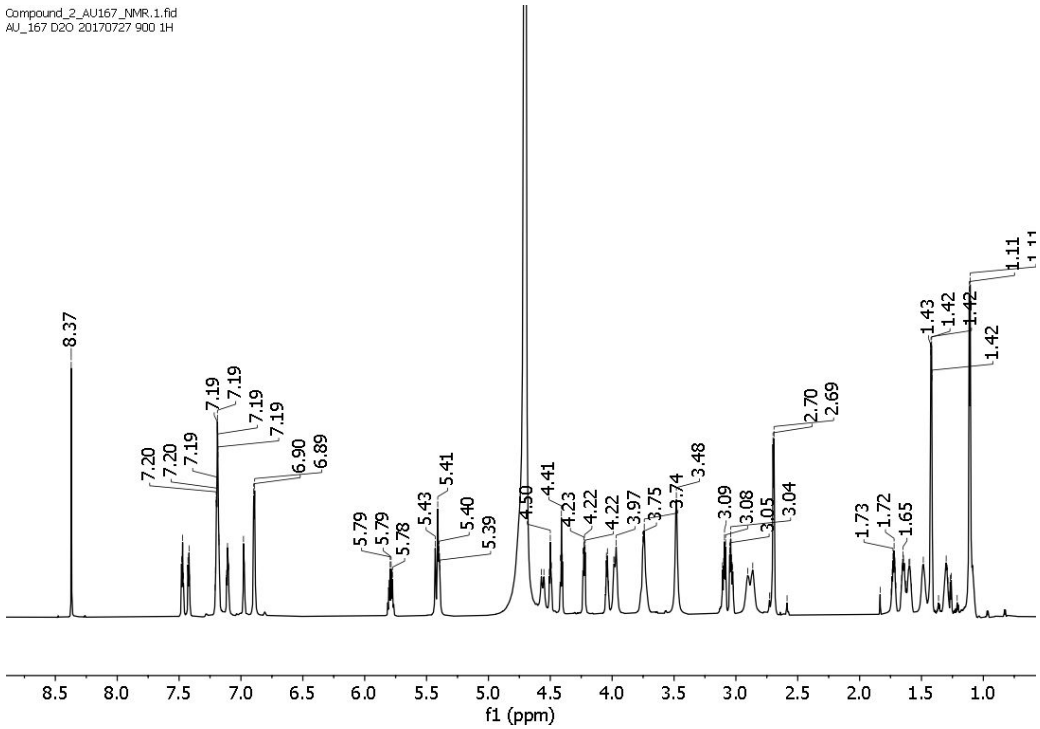

Figure S14. The ^{1}H NMR spectrum of compound **2** acquired at 800 MHz, 25 °C in D_2O.

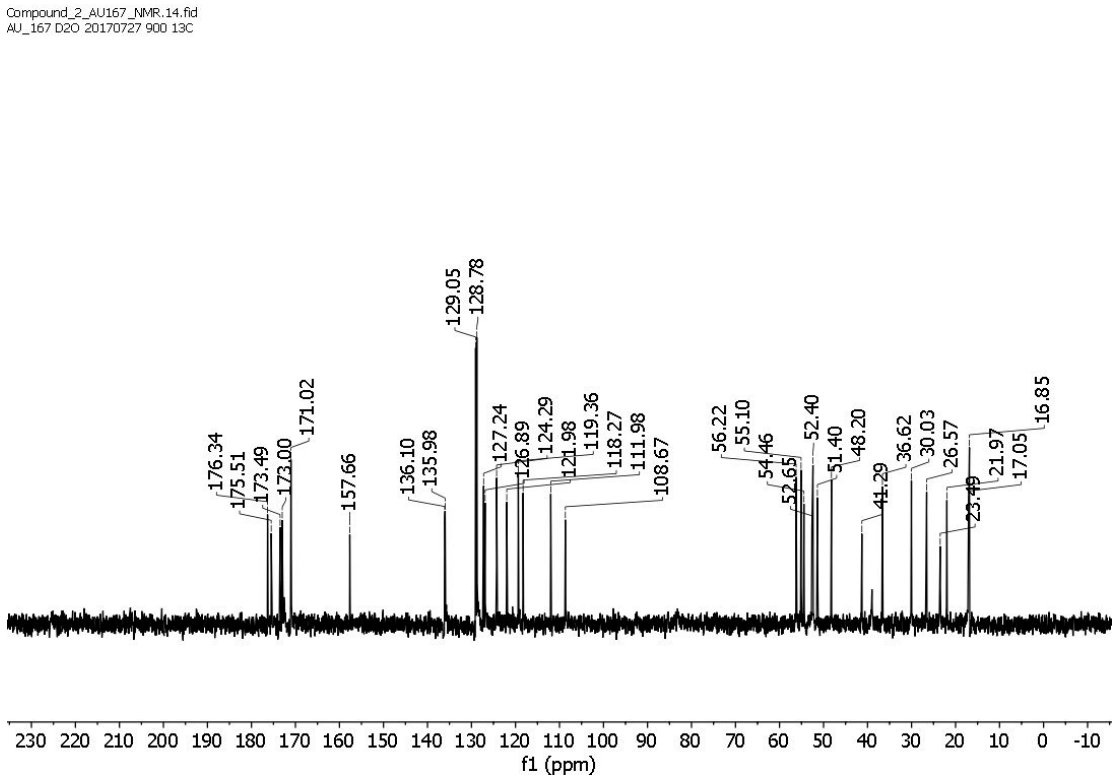

Figure S15. The ^{13}C NMR spectrum of compound **2** acquired at 800 MHz, 25 °C in D_2O.

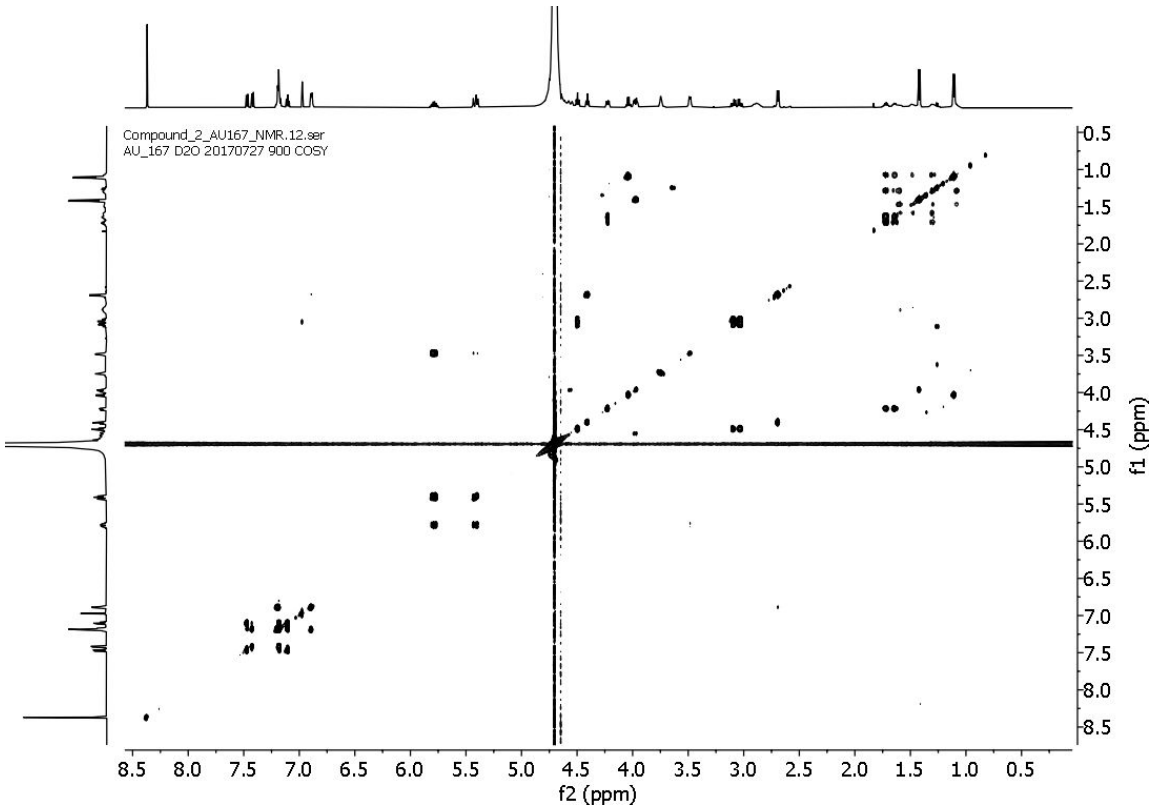

Figure S16. The COSY spectrum of compound **2** acquired at 800 MHz, 25 °C in D_2O.

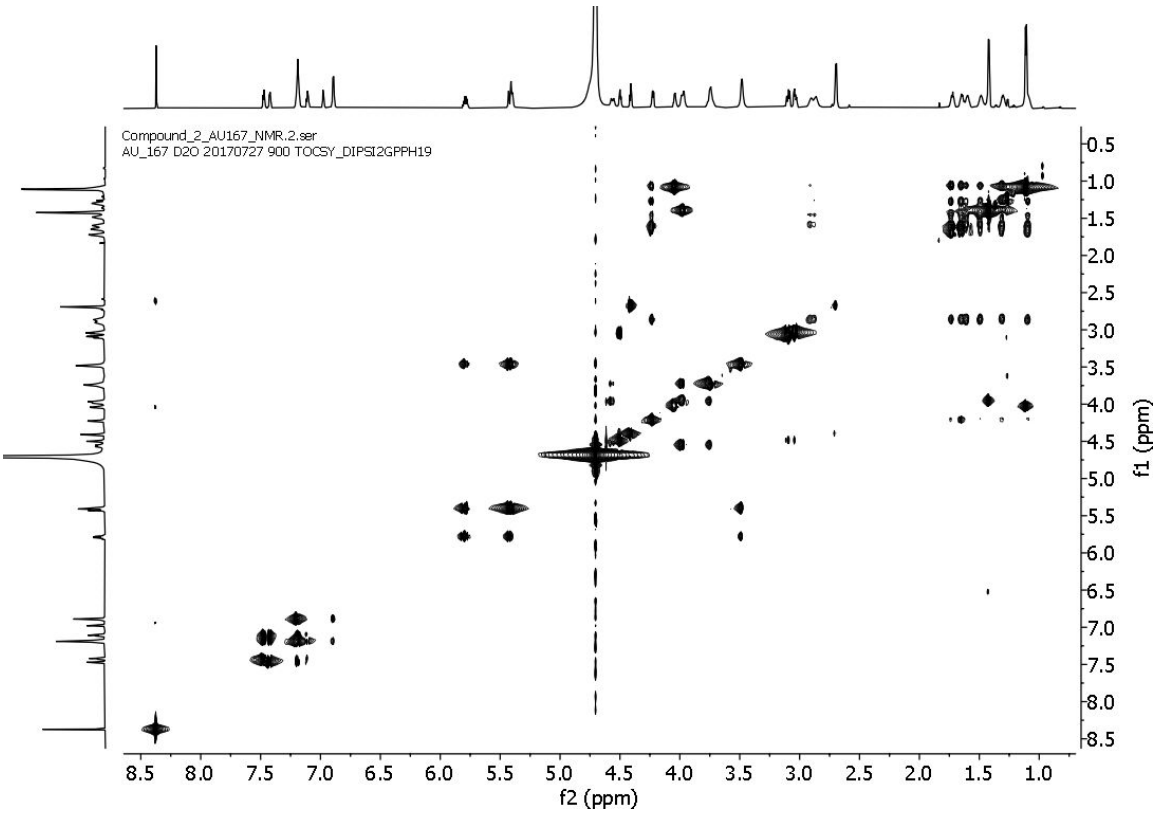

Figure S17. The TOCSY spectrum of compound **2** acquired at 800 MHz, 25 °C in D_2O.

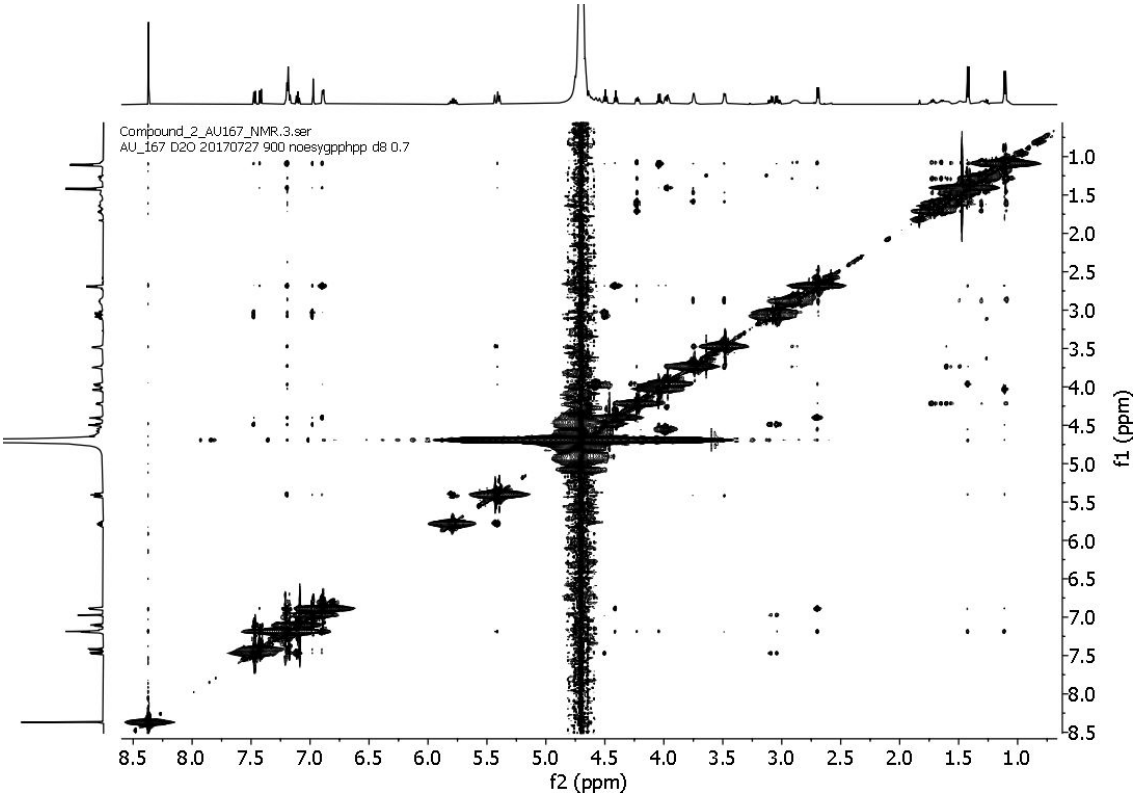

Figure S18. The NOESY spectrum of compound **2** acquired at 900 MHz, 25 °C in D_2O ,d_1=2.5 and mix =0.7 s.

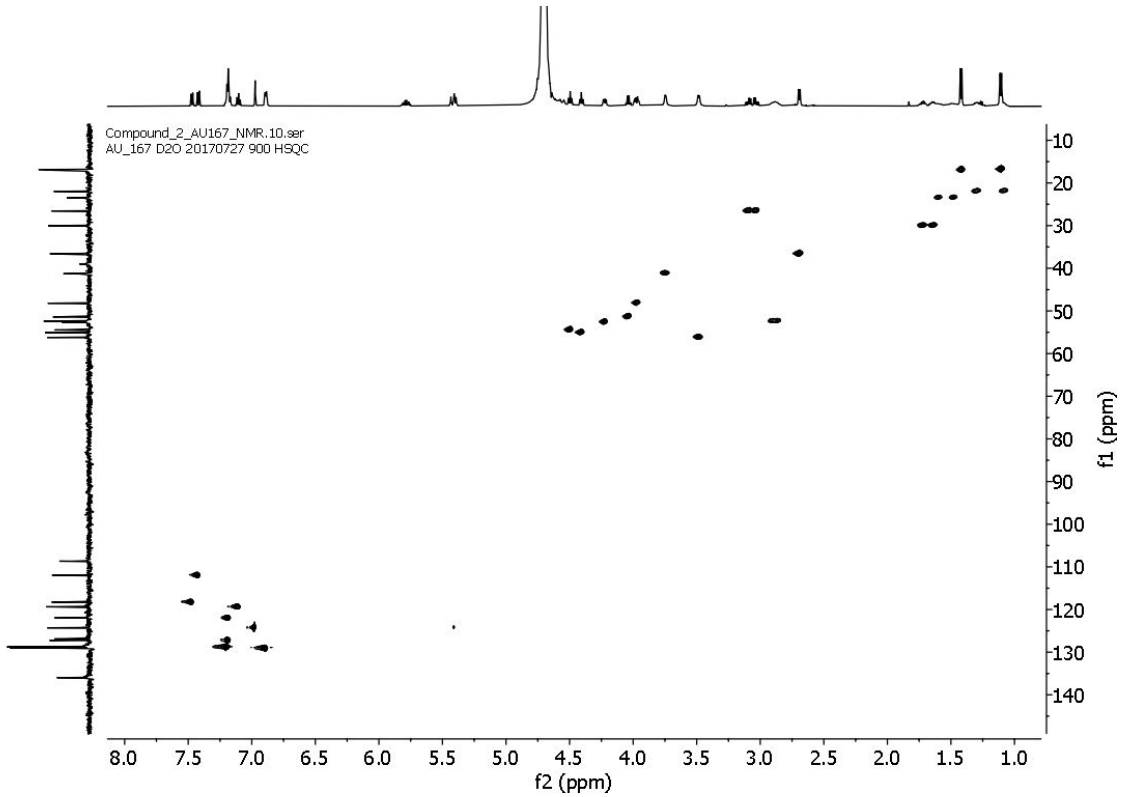

Figure S19. The HSQC spectrum of compound **2** acquired at 800/200 MHz, 25 °C in D_2O.

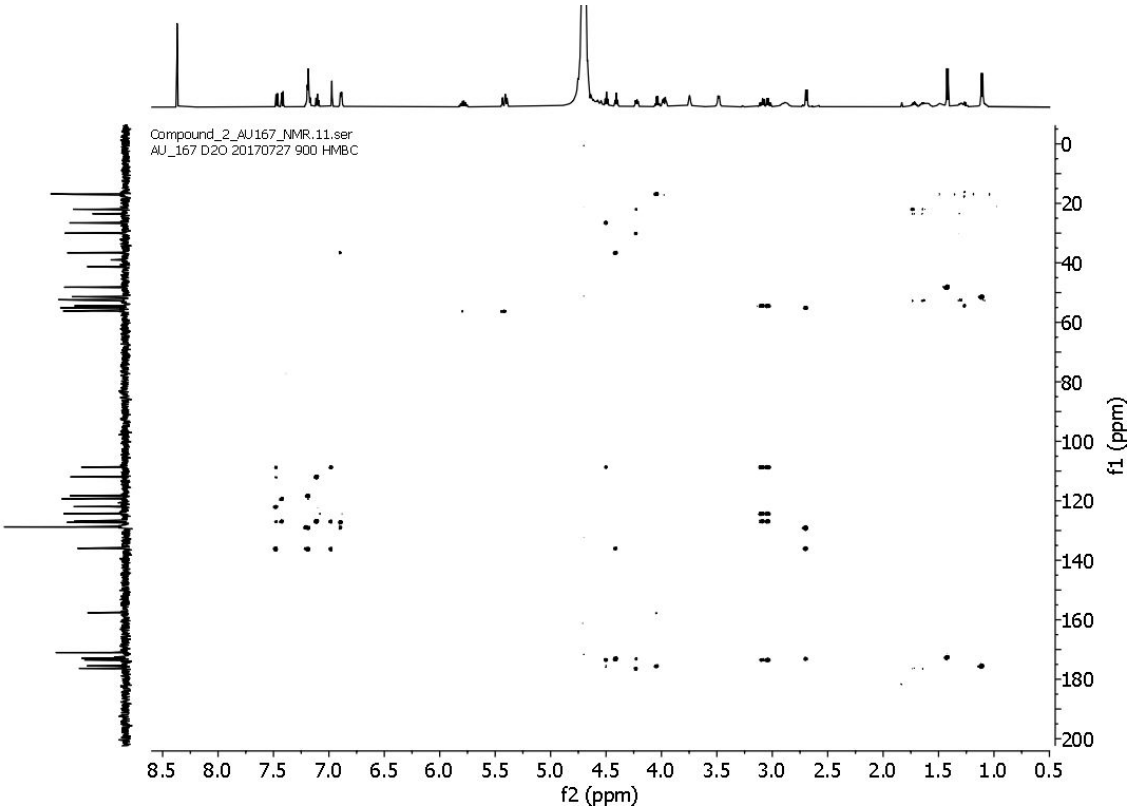

Figure S20. The HMBC spectrum of compound **2** acquired at 800/200 MHz, 25 °C in D_2O.

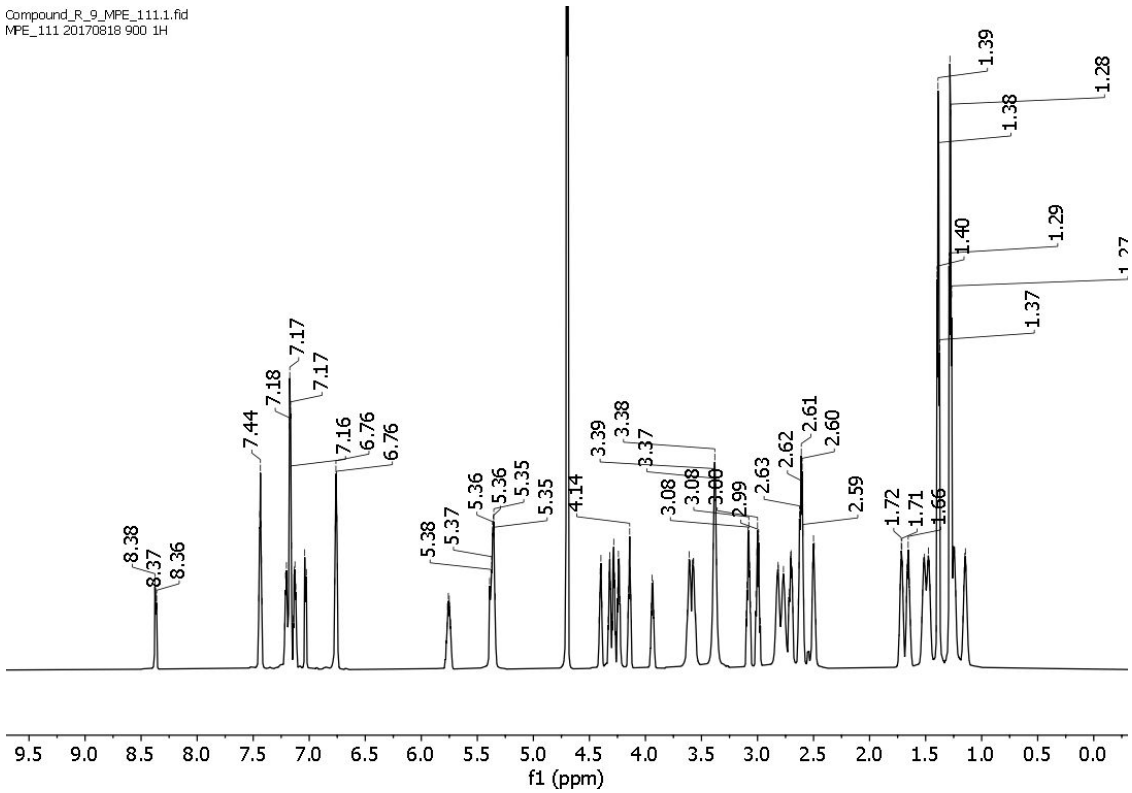

Figure S21. The ^{1}H NMR spectrum of compound **(S)-9** acquired at 900 MHz, 25 °C in D_2O.

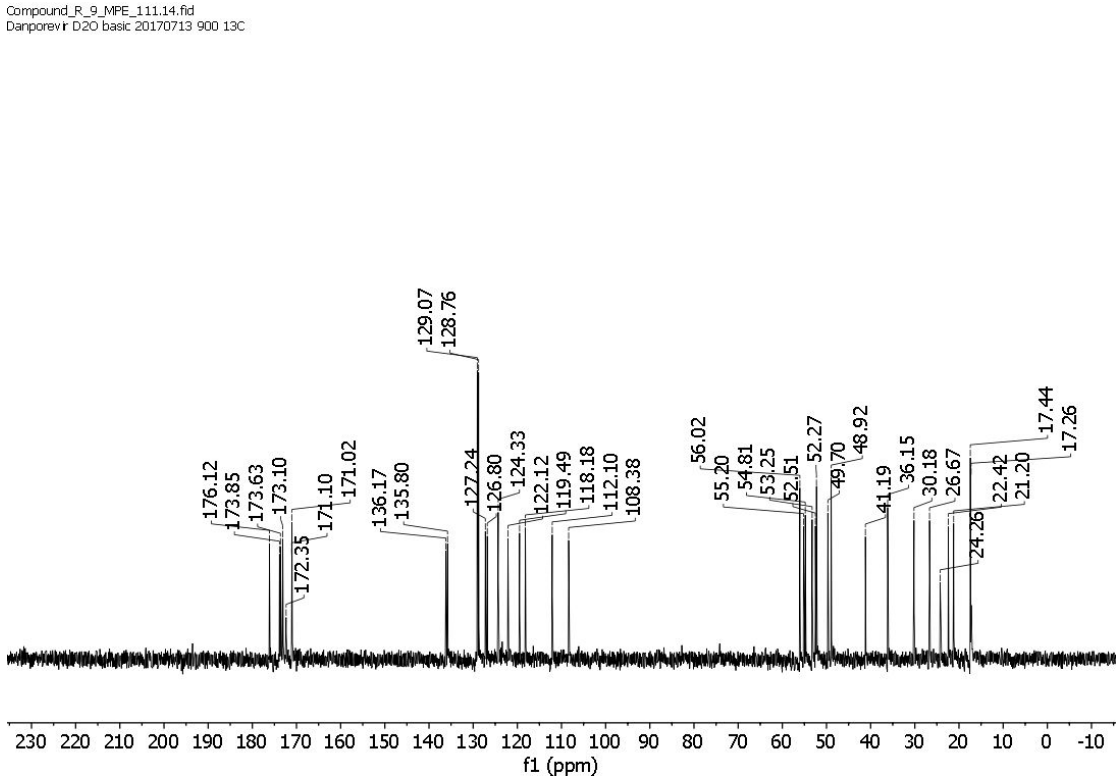

Figure S22. The ^{13}C NMR spectrum of compound **(S)-9** acquired at 225 MHz, 25 °C in D_2O.

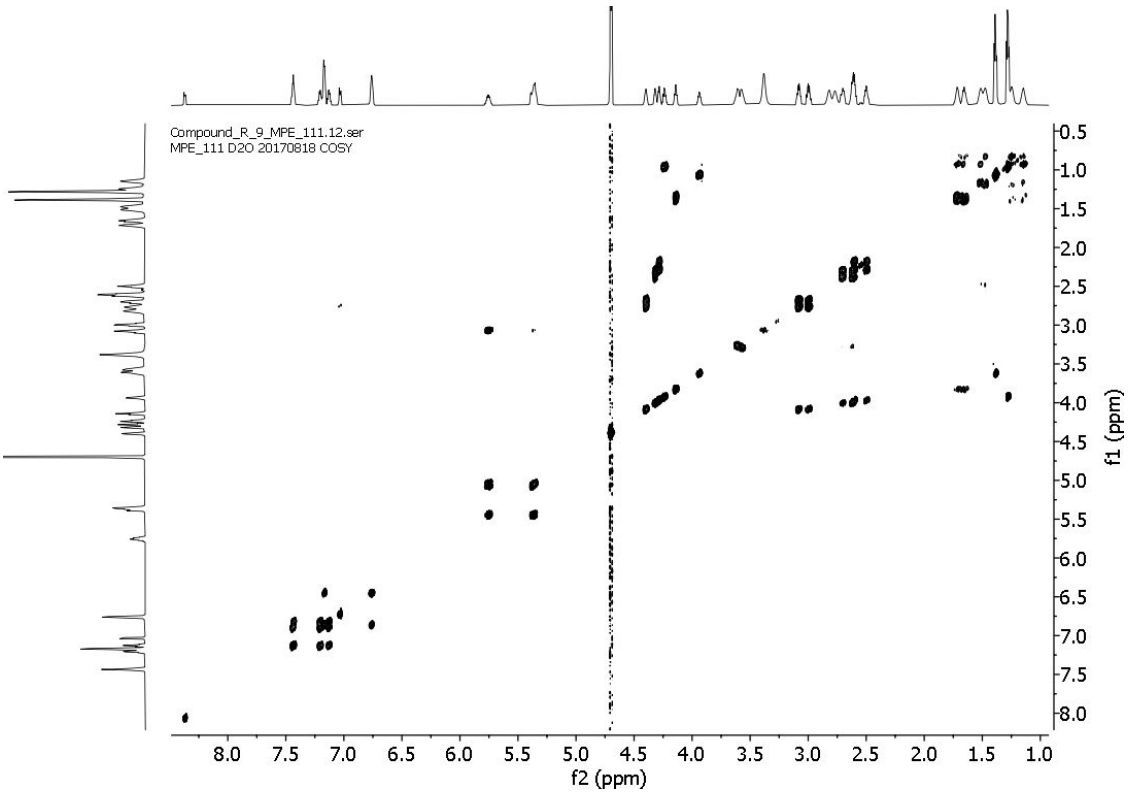

Figure S23. The COSY spectrum of compound **(S)-9** acquired at 900 MHz, 25 °C in D_2O.

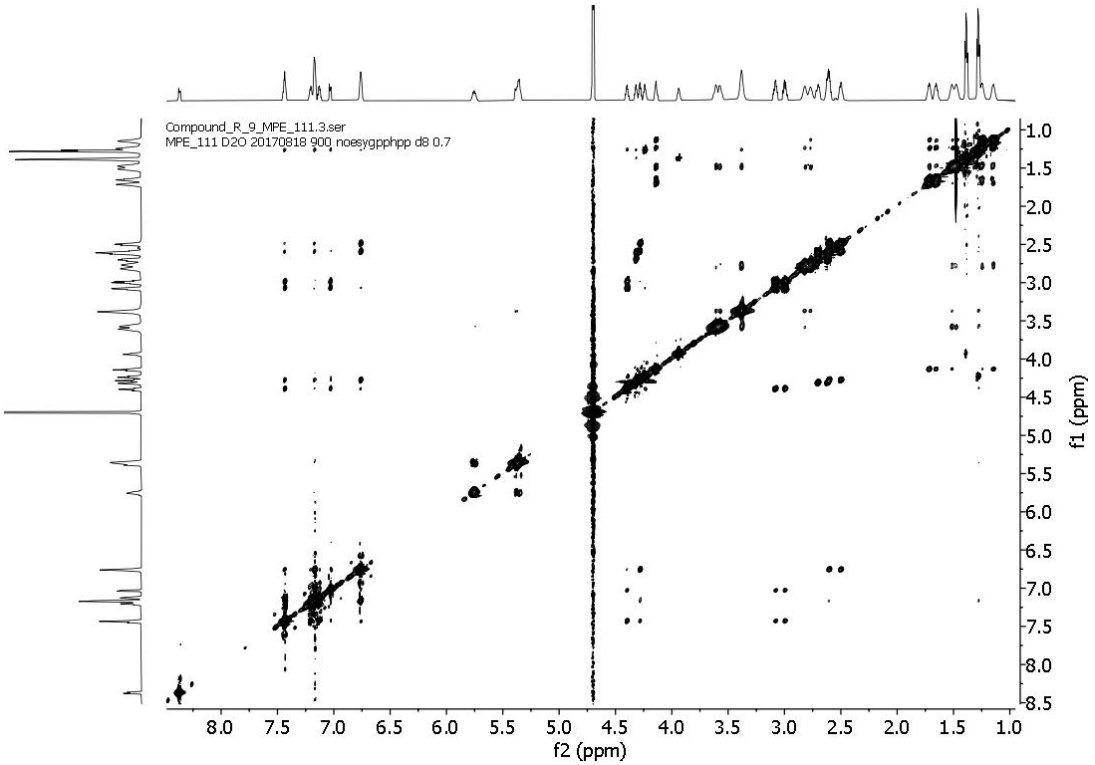

Figure S24. The NOESY spectrum of compound **(S)-9** acquired at 900 MHz, 25 °C in D_2O ,d_1=2.5 and mix =0.7 s.

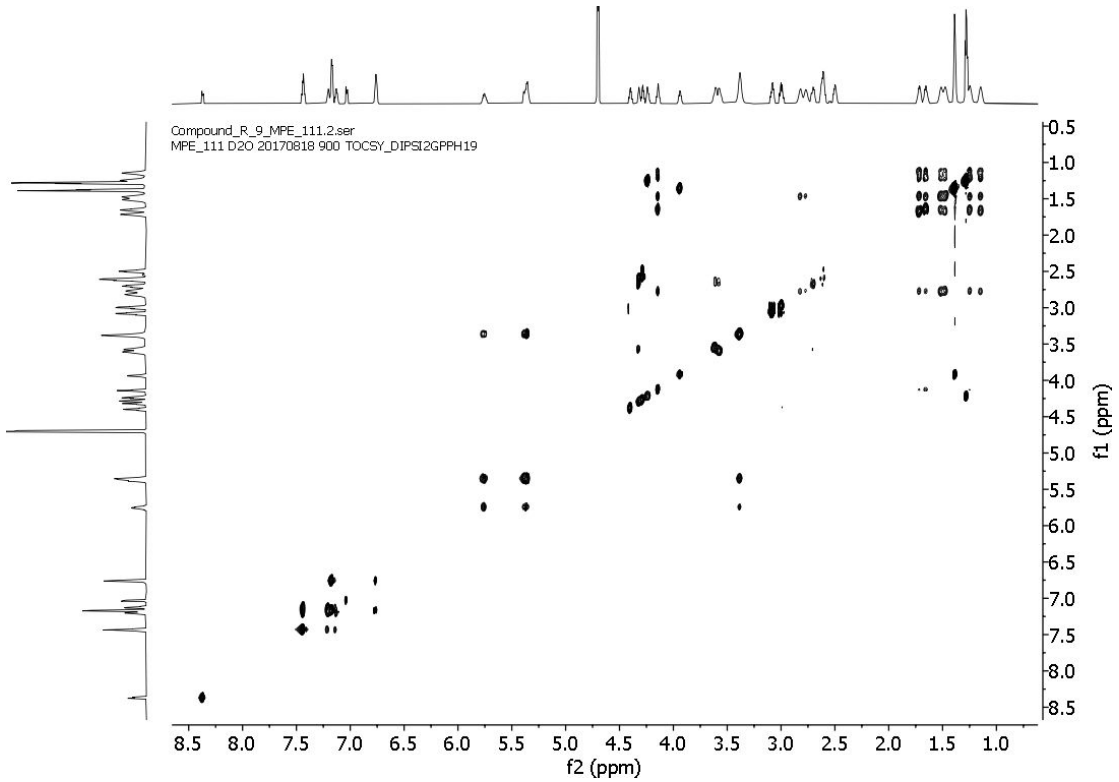

Figure S25. The TOCSY spectrum of compound **(S)-9** acquired at 900 MHz, 25 °C in D_2O.

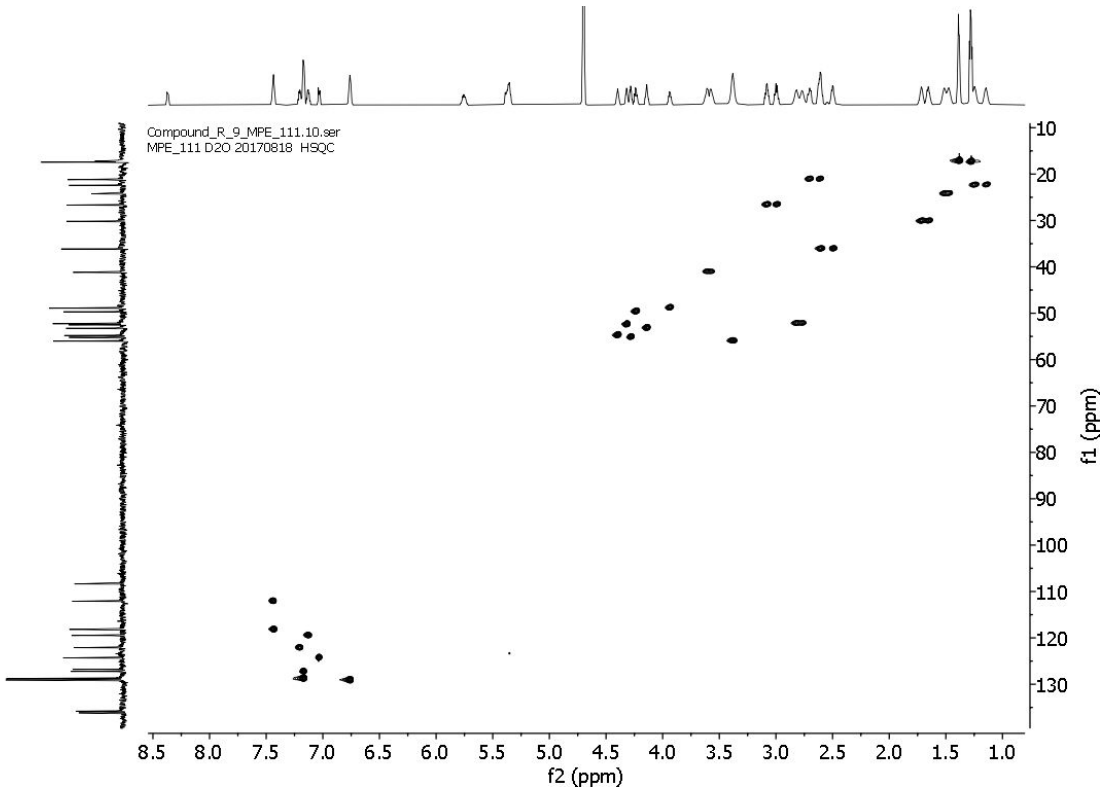

Figure S26. The HSQC spectrum of compound **(S)-9** acquired at 800/225 MHz, 25 °C in D_2O.

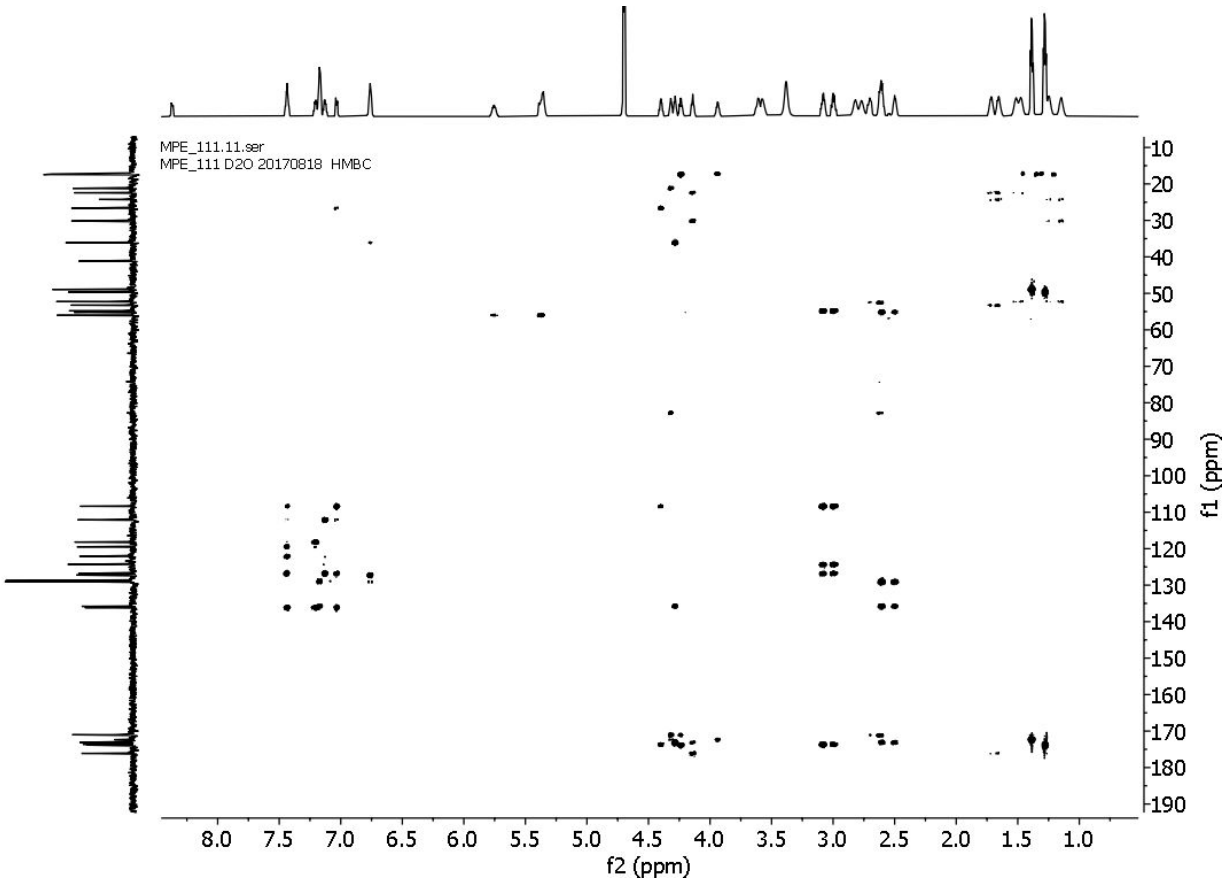

Figure S27. The HMBC spectrum of compound (**S**)-**9** acquired at 900/225 MHz, 25 °C in D_2O.

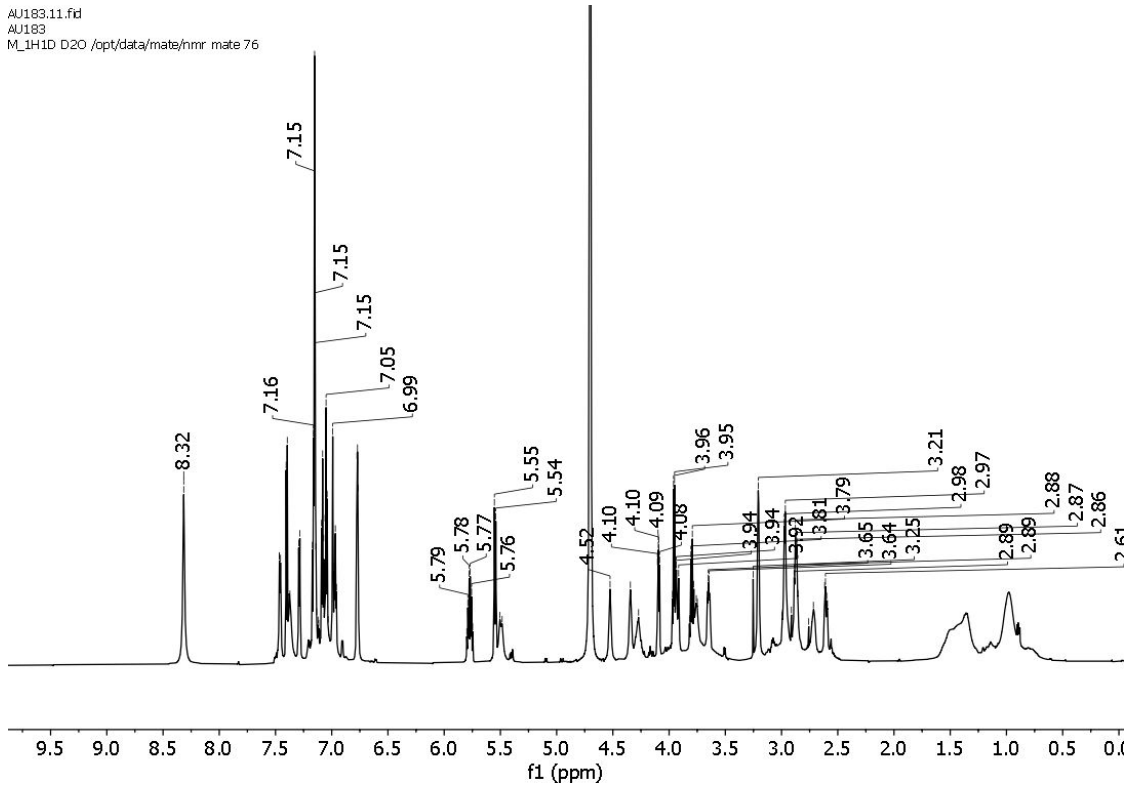

Figure S28. The ^{1}H NMR spectrum of compound **10** acquired at 800 MHz, 25 °C in D_2O.

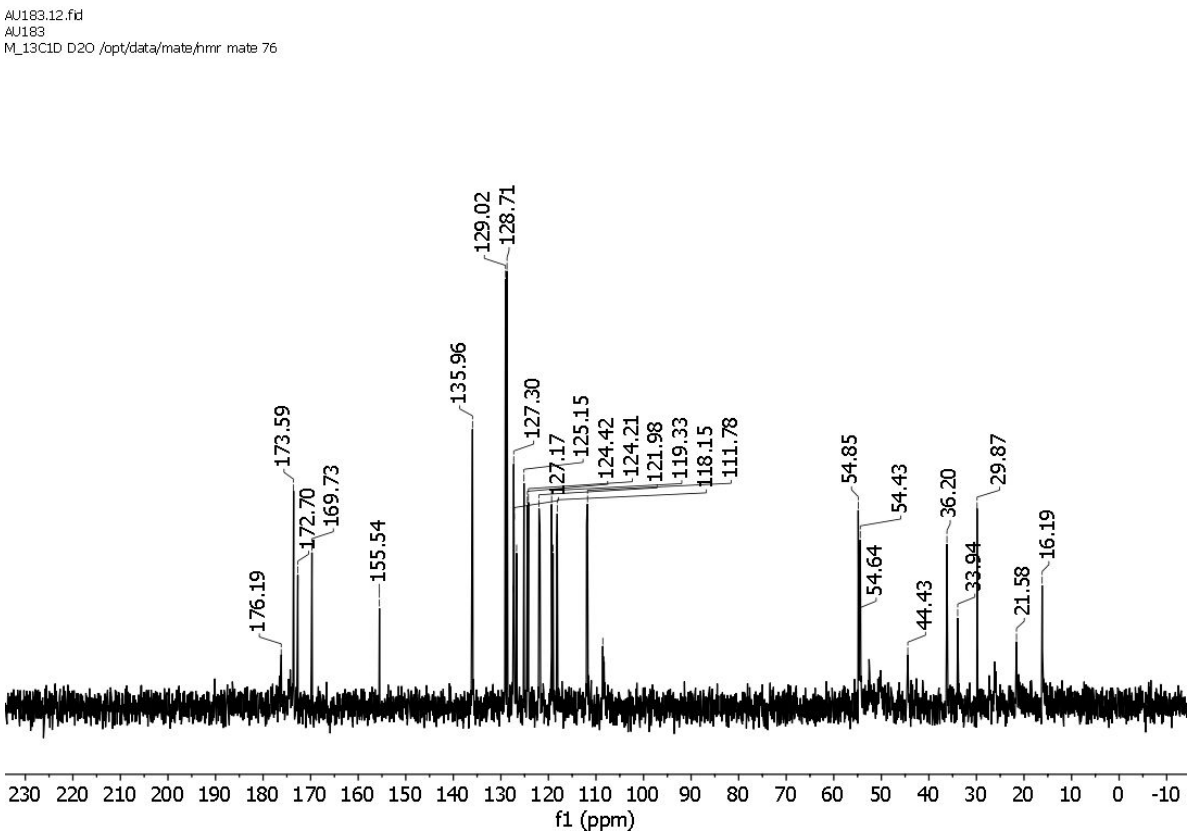

Figure S29. The ^{13}C NMR spectrum of compound **10** acquired at 200 MHz, 25 °C in D_2O.

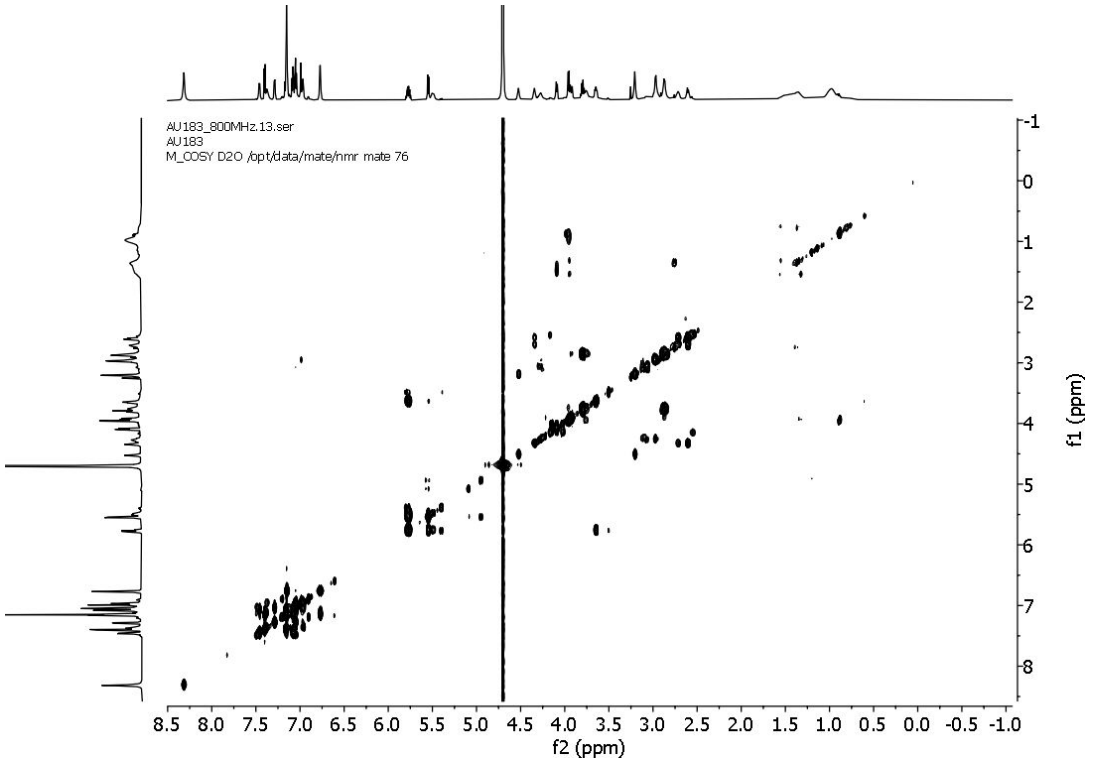

Figure S30. The COSY spectrum of compound **10** acquired at 800 MHz, 25 °C in D_2O.

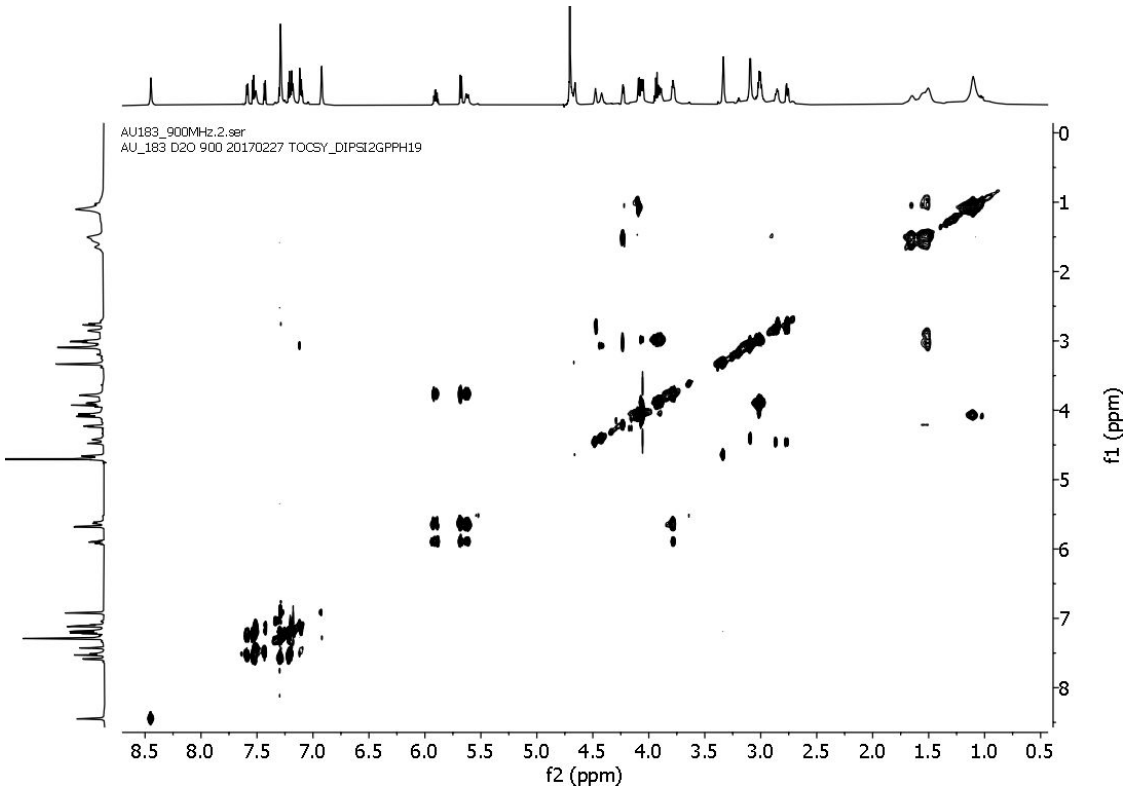

Figure S31. The TOCSY spectrum of compound **10** acquired at 900 MHz, 25 °C in D_2O.

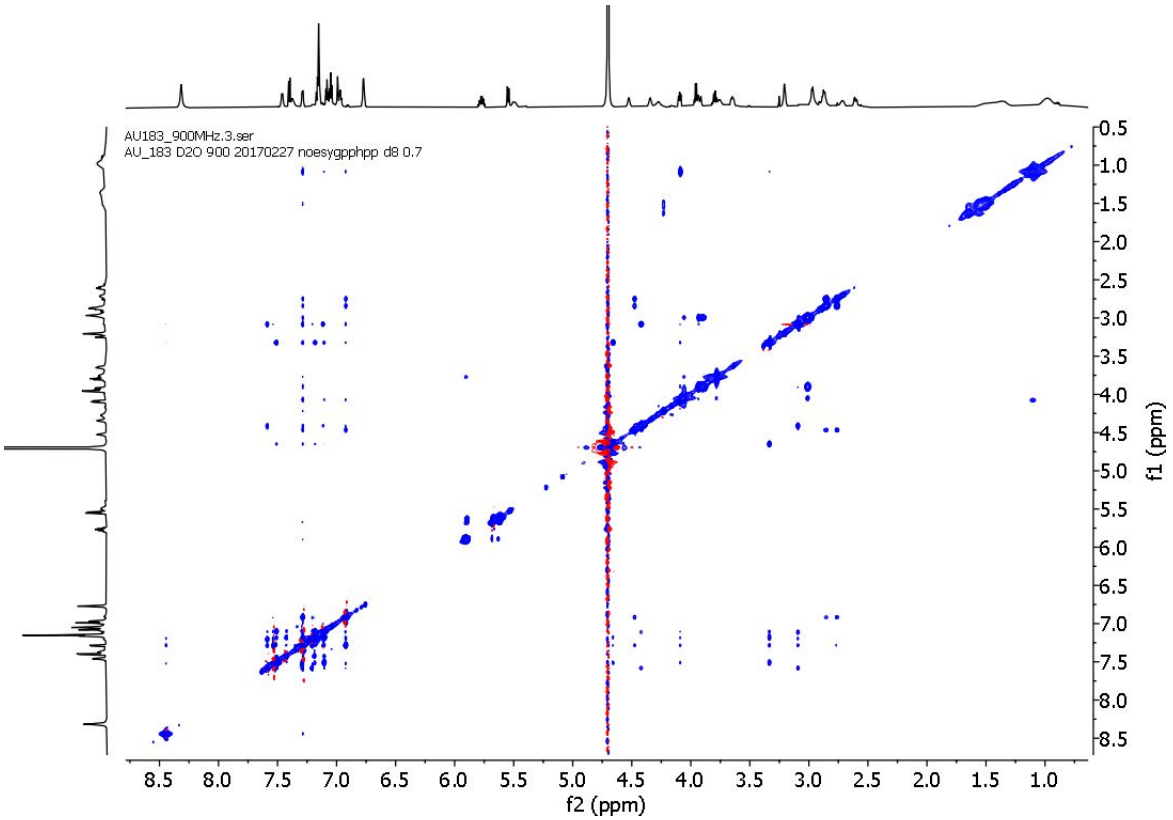

Figure S32. The NOESY spectrum of compound **10** acquired at 900 MHz, 25 °C in D_2O ,d_1=2.5 and mix =0.7 s.

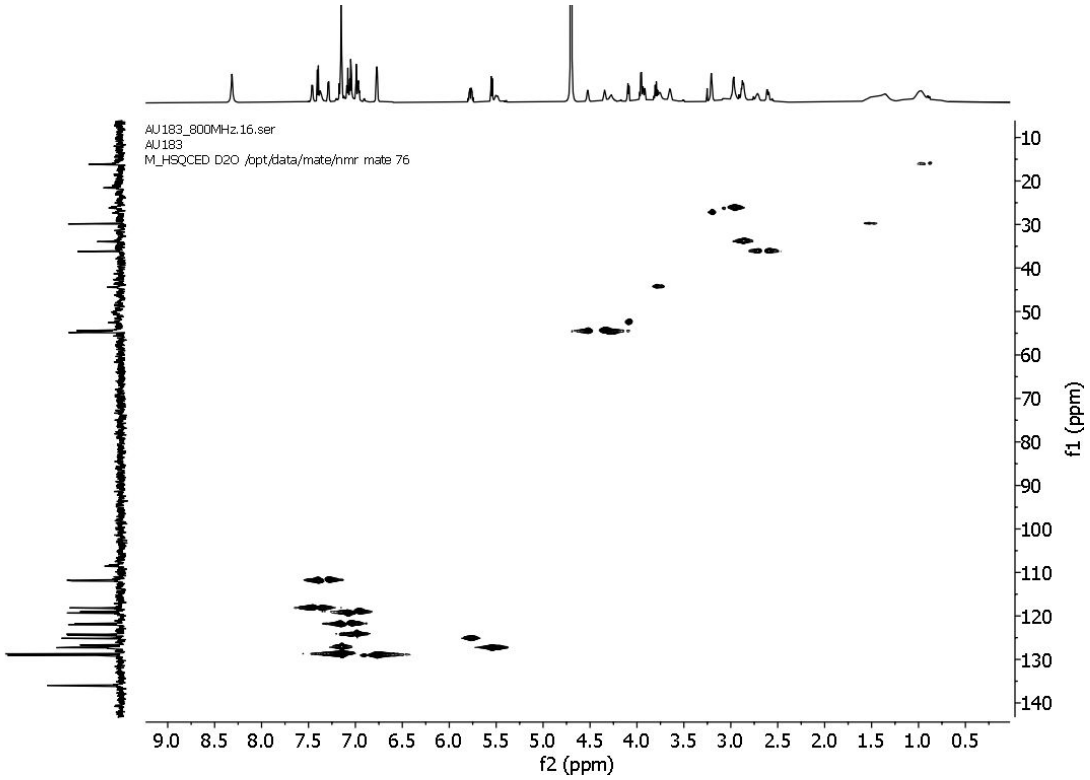

Figure S33. The HSQC spectrum of compound **10** acquired at 800/200 MHz, 25 °C in D_2O.

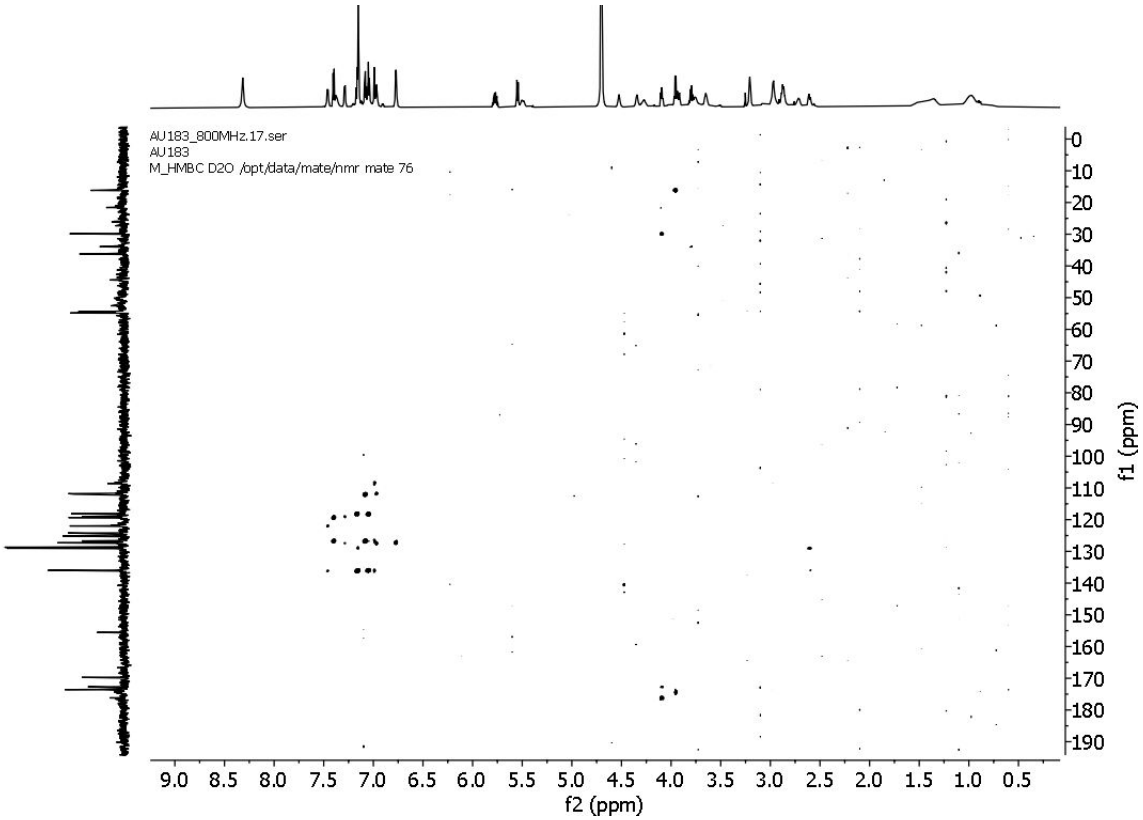

Figure S34. The HMBC spectrum of compound **10** acquired at 800/200 MHz, 25 °C in D_2O.

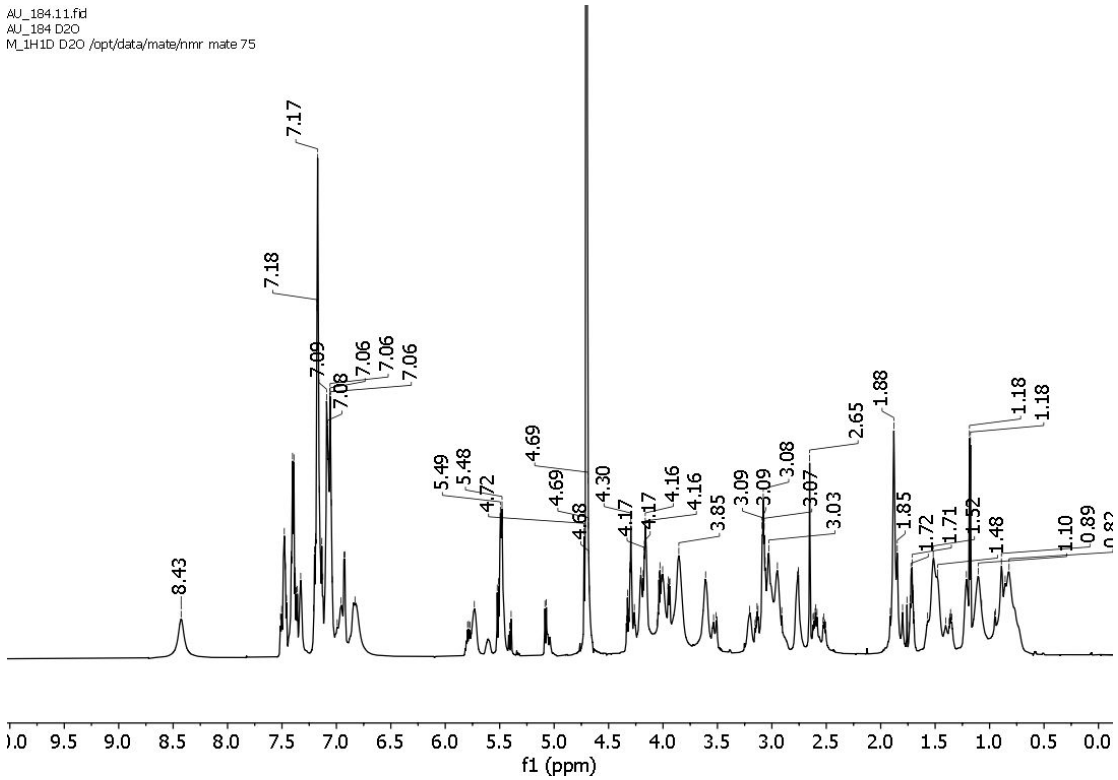

Figure S35. The ^{1}H NMR spectrum of compound **11** acquired at 800 MHz, 25 °C in D_2O.

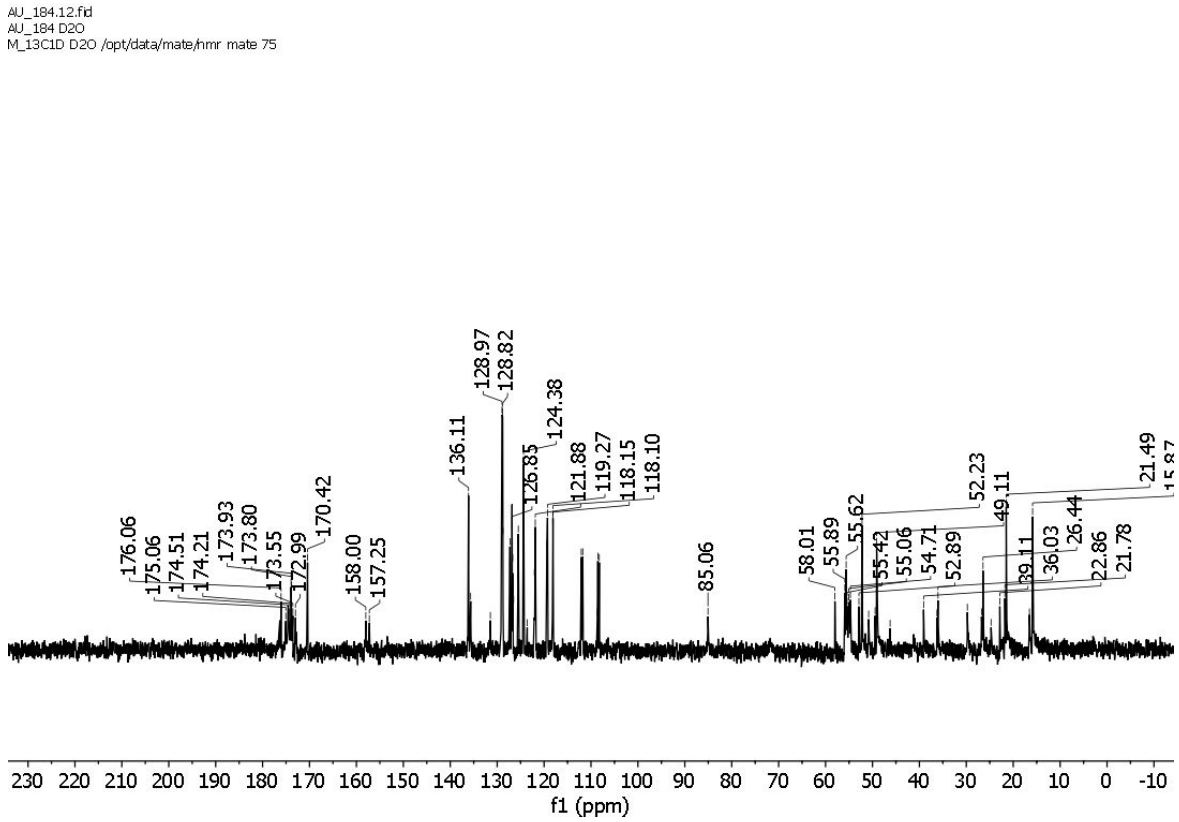

Figure S36. The ^{13}C NMR spectrum of compound **11** acquired at 800 MHz, 25 °C in D_2O.

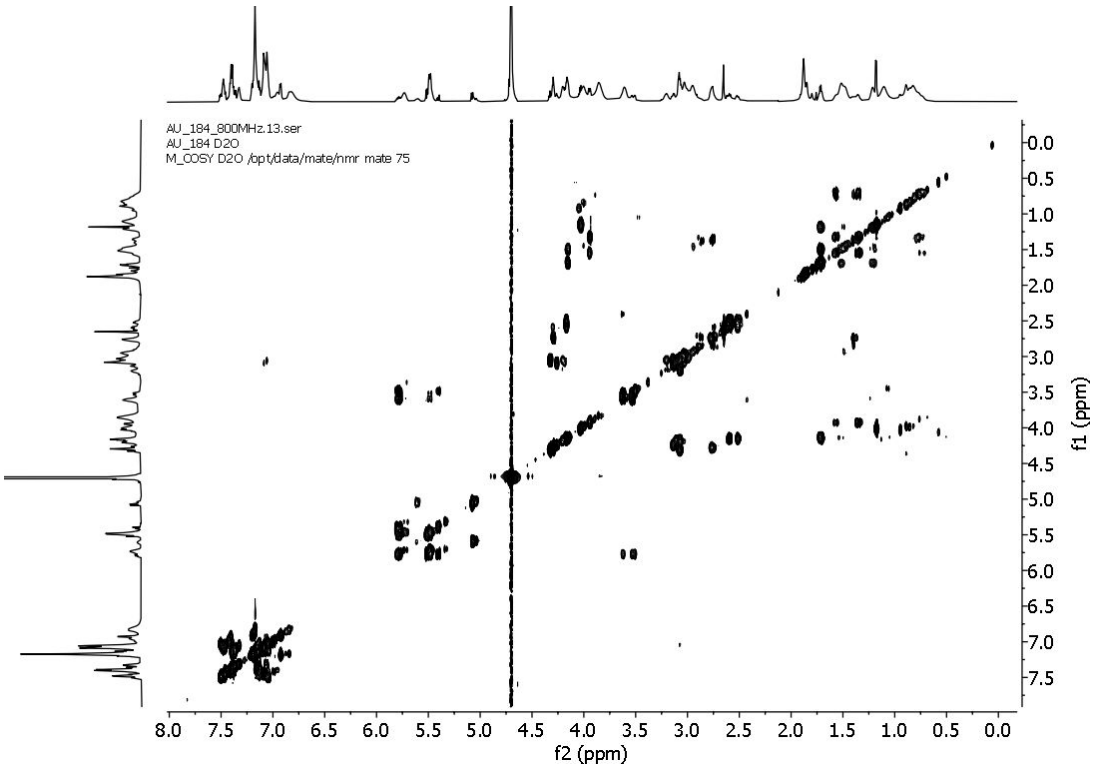

Figure S37. The COSY spectrum of compound **11** acquired at 800 MHz, 25 °C in D_2O.

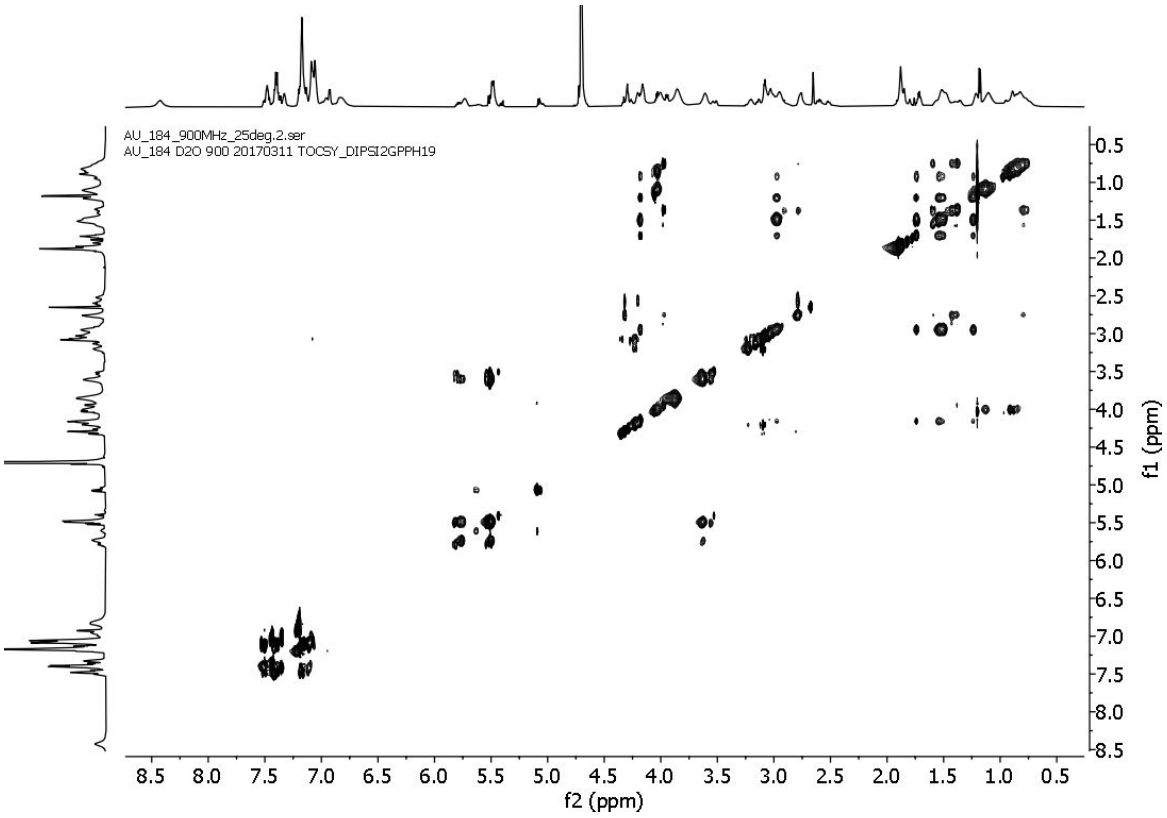

Figure S38. The TOCSY spectrum of compound **11** acquired at 800 MHz, 25 °C in D_2O.

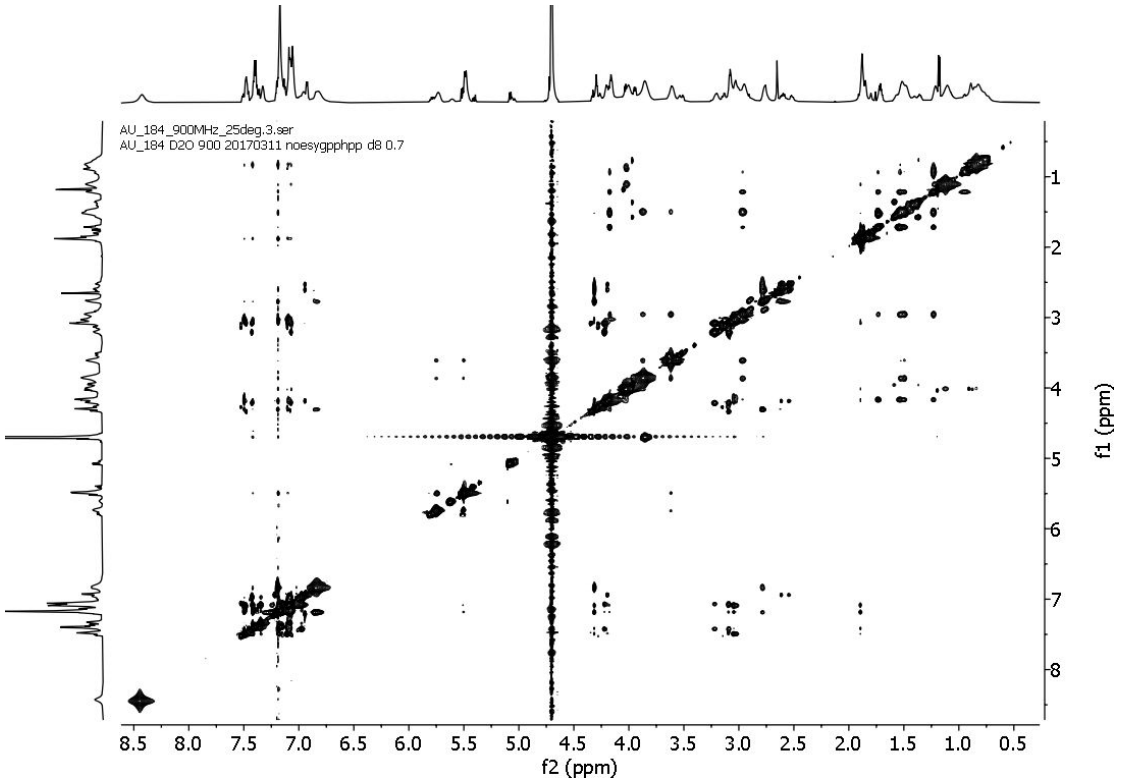

Figure S39. The NOESY spectrum of compound **11** acquired at 900 MHz, 25 °C in D_2O ,d_1=2.5 and mix =0.7 s.

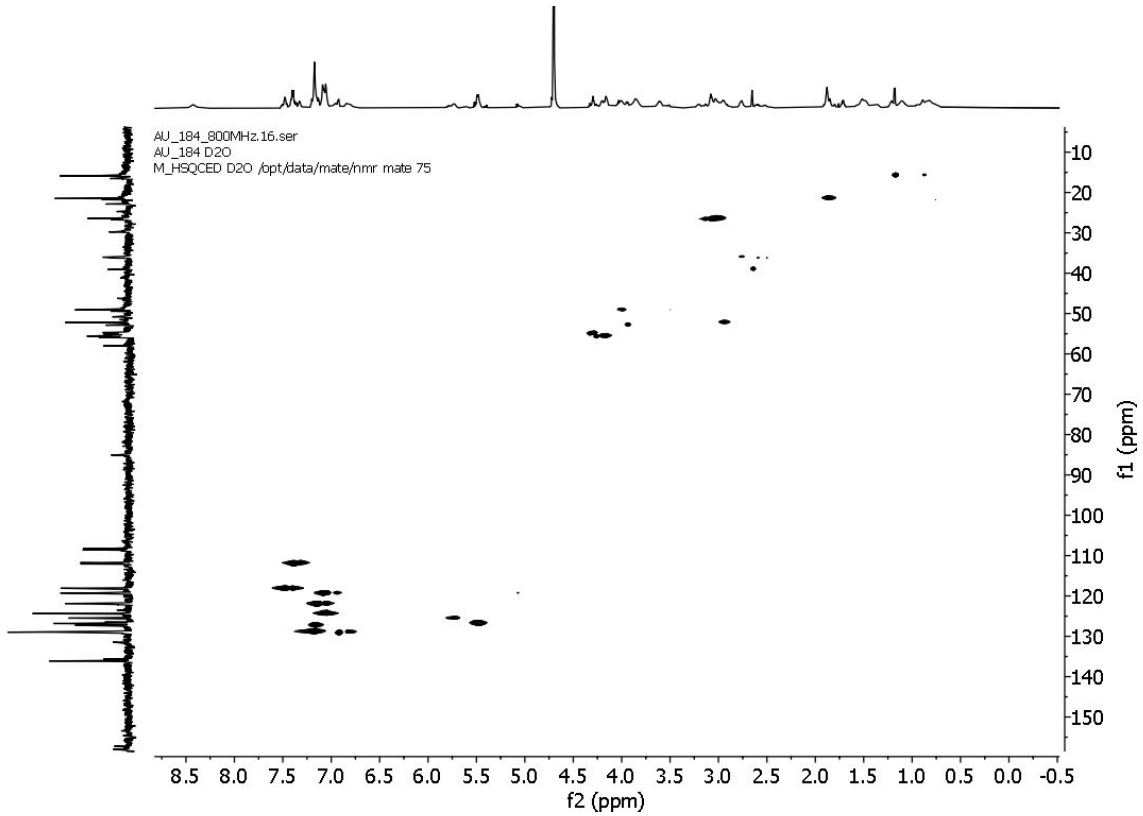

Figure S40. The HSQC spectrum of compound **11** acquired at 800/200 MHz, 25 °C in D_2O.

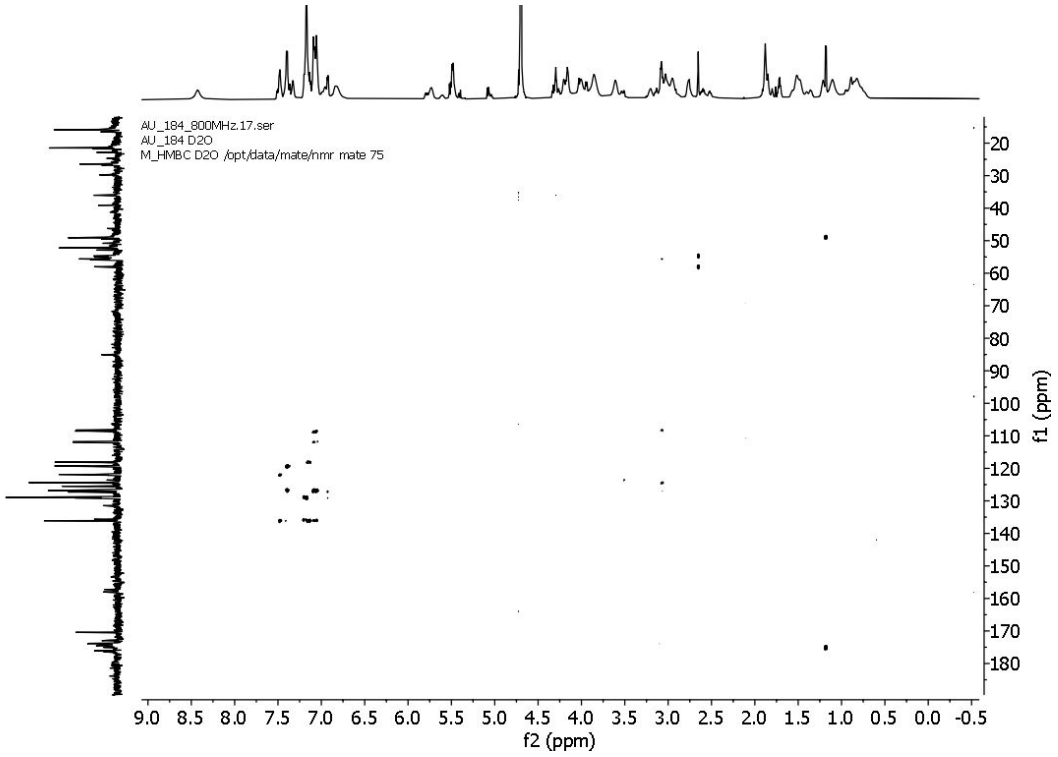

Figure S41. The HMBC spectrum of compound **11** acquired at 800/200 MHz, 25 °C in D_2O.

References

(1) Zhang, J.; Mulumba, M.; Ong, H.; Lubell, W. D. Diversity-Oriented Synthesis of Cyclic Azapeptides by A3-Macrocyclization Provides High-Affinity CD36-Modulating Peptidomimetics. *Angew. Chemie Int. Ed.* **2017**, *56* (22), 6284–6288.

(2) Clark Still, W.; Tempczyk, A.; Hawley, R. C.; Hendrickson, T. Semianalytical Treatment of Solvation for Molecular Mechanics and Dynamics. *J. Am. Chem. Soc.* **1990**, *112* (16), 6127–6129.

(3) Nevins, N.; Cicero, D.; Snyder, J. P. A Test of the Single-Conformation Hypothesis in the Analysis of NMR Data for Small Polar Molecules: A Force Field Comparison. *J. Org. Chem.* **1999**, *64* (11), 3979–3986.

(4) Mohamadi, F.; Richards, N. G. J.; Guida, W. C.; Liskamp, R.; Lipton, M.; Caufield, C.; Chang, G.; Hendrickson, T.; Still, W. C. Macromodel—an Integrated Software System for Modeling Organic and Bioorganic Molecules Using Molecular Mechanics. *J. Comput. Chem.* **1990**, *11* (4), 440–467.

(5) Cicero, D., O.; Barbato, G.; Bazzo, R. NMR Analysis of Molecular Flexibility in Solution : A New Method for the Study of Complex Distributions of Rapidly Exchanging Conformations. Application to a 13-Residue Peptide with an 8-Residue Loop. *J. Am. Chem. Soc.* **1995**, *117* (3), 1027–1033.

(6) Aike, H. A New Look at the Statistical Model Identification. *IEEE Trans. Automat. Contr.* **1974**, *19* (6), 716–723.

(7) Auvergne, E. J.; Gooley, P. R. The Use of Model Selection in the Model-Free Analysis of Protein Dynamics. *J. Biomol. NMR* **2003**, *25*, 25–39.

(8) Kass, R. E.; Raftery, A. E. Bayes Factors. *J. Am. Stat. Assoc.* **1995**, *90*, 773–795.